Nuclear structure imaging in high-energy nuclear collisions

Jiangyong Jia

Stony Brook University | The State University of New York

07/24/2023, summer school lecture

Landscape of nuclear physics

Quark-gluon plasma

hadrons

nuclei

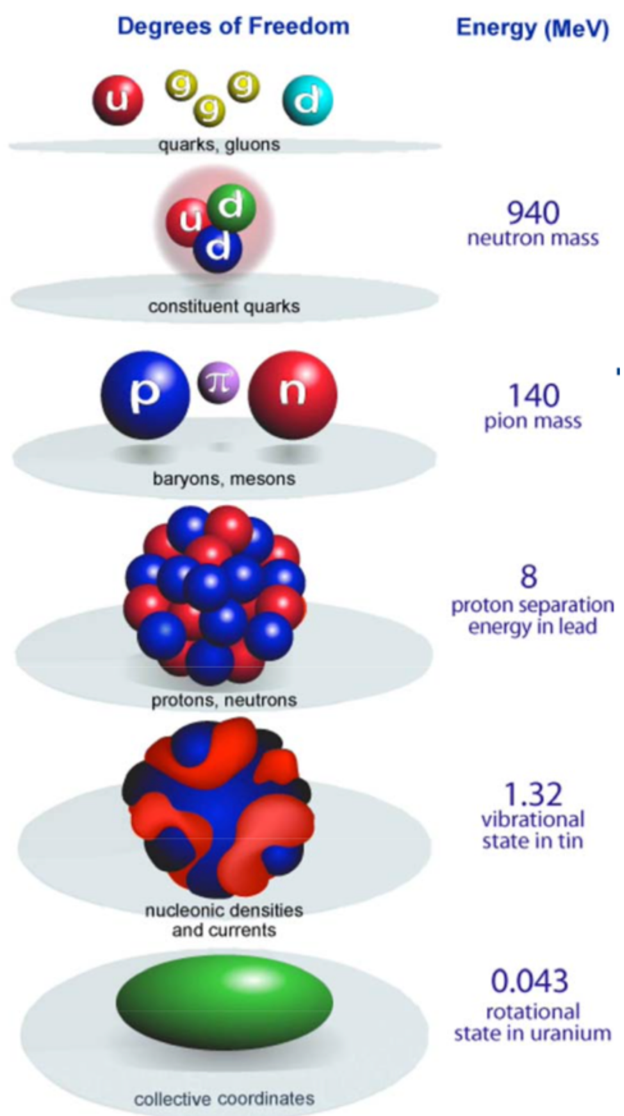

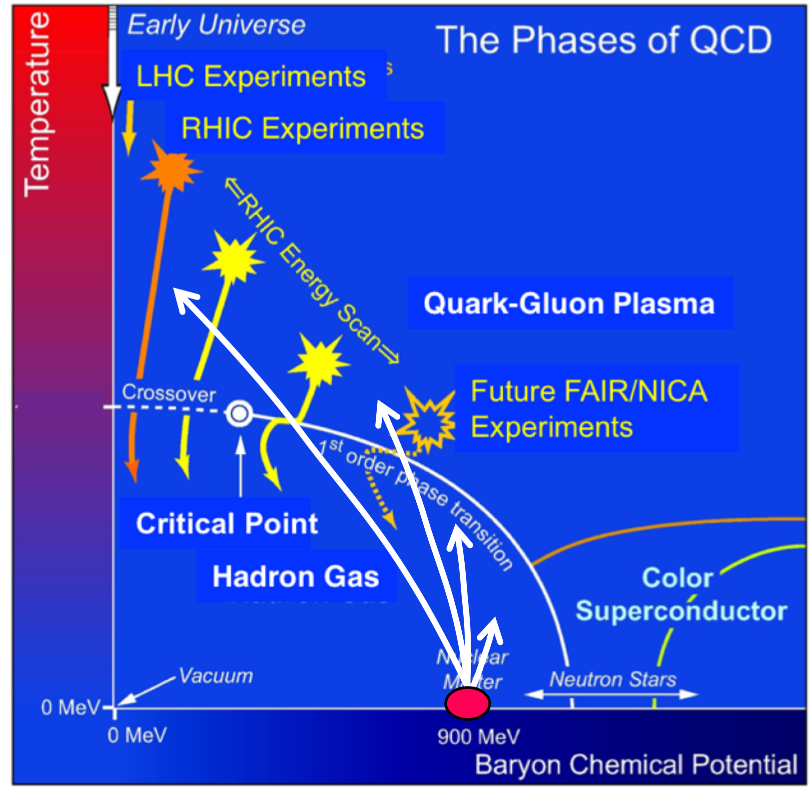

Most nuclear experiments starts with nuclei

Collective shape of atomic nuclei

- Emergent phenomena of many-body quantum system
  - clustering, halo, skin, bubble…
  - quadrupole/octupole/hexdecopole deformation
  - Nontrivial evaluation with N and Z.

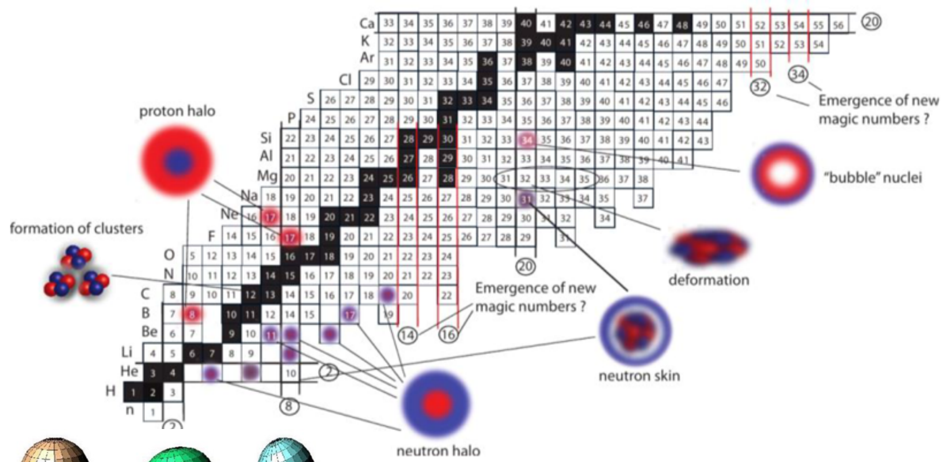

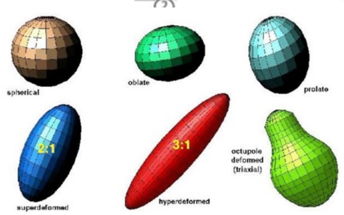

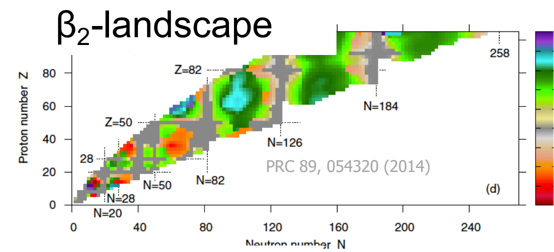

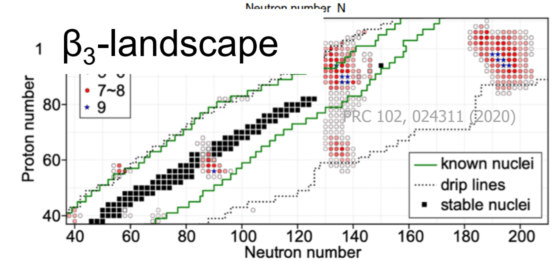

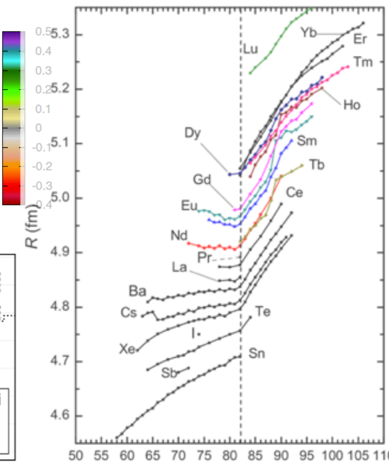

PRC 89, 054320 (2014)

$$\rho(r,\theta,\phi) = \frac{\rho_0}{1+e^{(r-R(\theta,\phi))/a_0}}$$

$$R(\theta,\phi) = R_0(1+\beta_2[\cos\gamma Y_{2,0}(\theta,\phi)+\sin\gamma Y_{2,2}(\theta,\phi)]+\beta_3 Y_{3,0}(\theta,\phi)+\beta_4 Y_{4,0}(\theta,\phi))$$

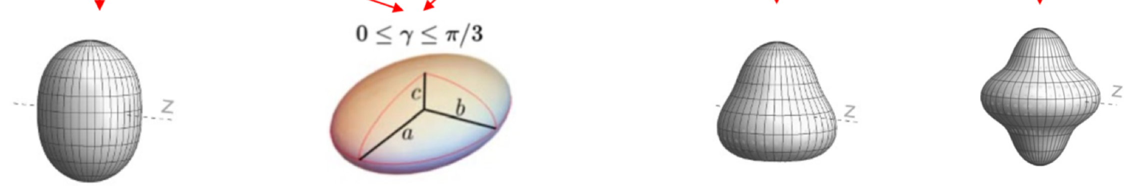

High-energy heavy ion collision

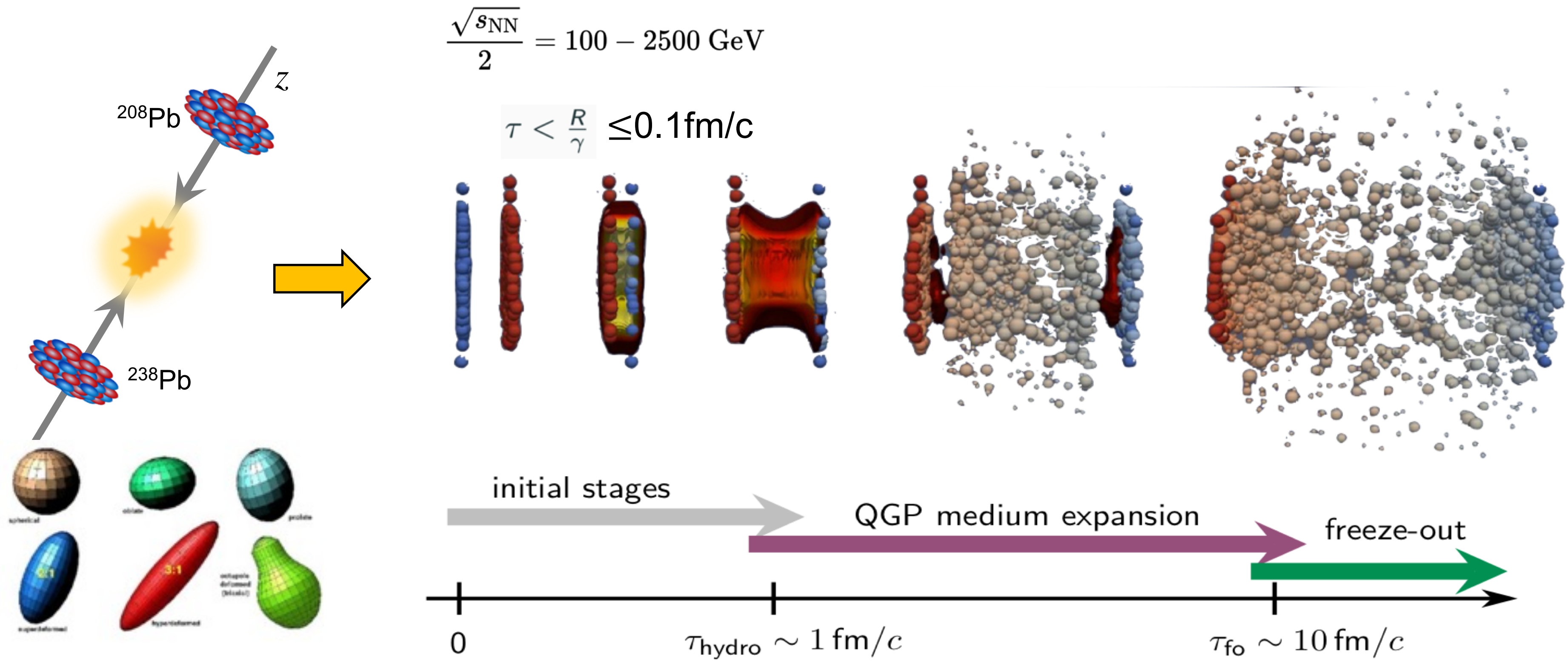

400 nucleons → 30000 hadrons

in 10^{-23} seconds

High-energy heavy ion collision

Nuclear structure | Initial condition | Final state

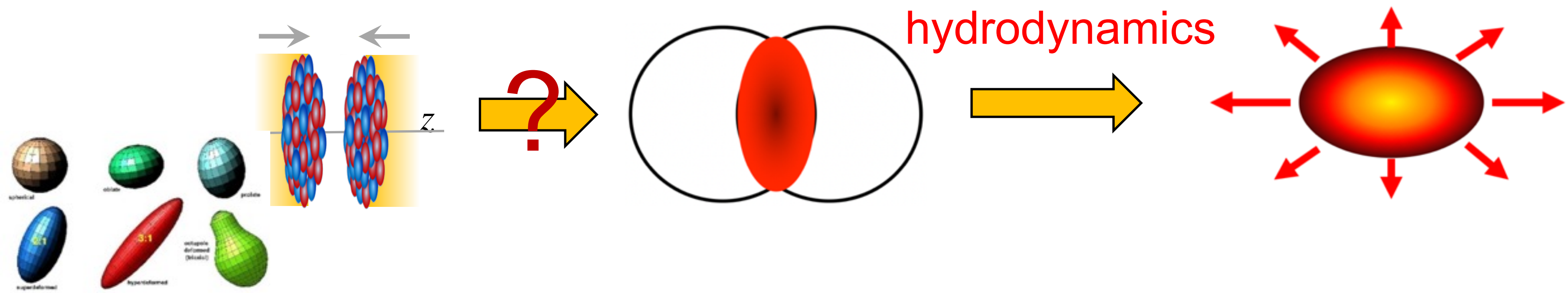

Shape and radial dis.

$\beta_2 \rightarrow$ Quadrupole deformation

$\beta_3 \rightarrow$ Octupole deformation

$a_0 \rightarrow$ Surface diffuseness

$R_0 \rightarrow$ Nuclear size

Volume, size and shape

N_{part}

$R_\perp^2 \propto \langle r_\perp^2 \rangle,$

$\mathcal{E}_n \propto \langle r_\perp^n e^{in\phi} \rangle$

Observables

$$\frac{d^2N}{d\phi dp_T} = N(p_T)\left(\sum_n V_n \, e^{-in\phi}\right)$$

Extraction of QGP properties is limited by the uncertainties in initial condition

- Comparing collisions of nuclei with different shapes constrains the initial condition
- Provide insights on manifestation of nuclear structure at high energy scale.

Infer initial condition from flow correlations

Initial state shape

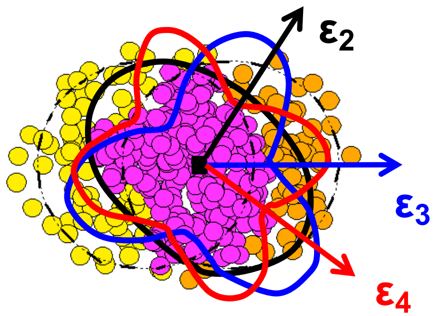

volume, size and shape

$N_{\rm part}$ $\quad R_\perp^2 \propto \langle r_\perp^2 \rangle,$ $\quad \mathcal{E}_2 \propto \left\langle r_\perp^2 e^{i2\phi} \right\rangle$

$\mathcal{E}_3 \propto \left\langle r_\perp^3 e^{i3\phi} \right\rangle$

$\mathcal{E}_4 \propto \left\langle r_\perp^4 e^{i4\phi} \right\rangle$

$\ldots$

$$F = -\nabla P(\epsilon)$$

Hydro-response

Final state flow

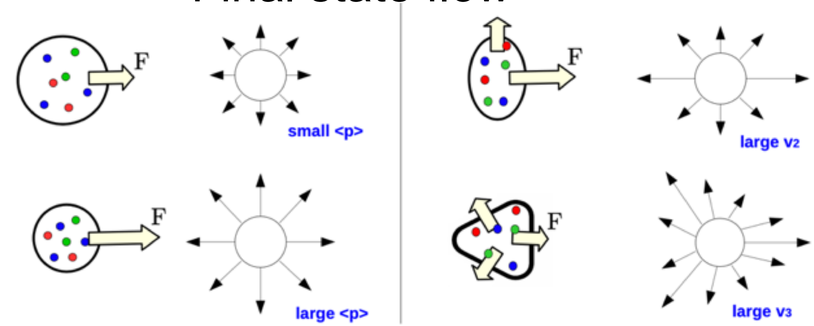

Multiplicity Radial Flow Harmonic Flow

$\mathrm{N_{ch}}$ $\quad \dfrac{d^2N}{d\phi dp_T} = N(p_T)\left(\sum_n V_n e^{-in\phi}\right)$

1206.1905

imaging relies on linear response:

$$\boxed{N_{ch} \propto N_{part} \quad \frac{\delta [p_T]}{[p_T]} \propto -\frac{\delta R_\perp}{R_\perp} \quad V_n \propto \mathcal{E}_n}$$

Connecting HI initial condition with nuclear shape

Body-Body $\qquad \mathcal{E}_2 = \epsilon_2 e^{i2\Phi} \propto \left\langle \boldsymbol{r}_\perp^2 e^{i2\phi} \right\rangle \qquad$ Tip-Tip

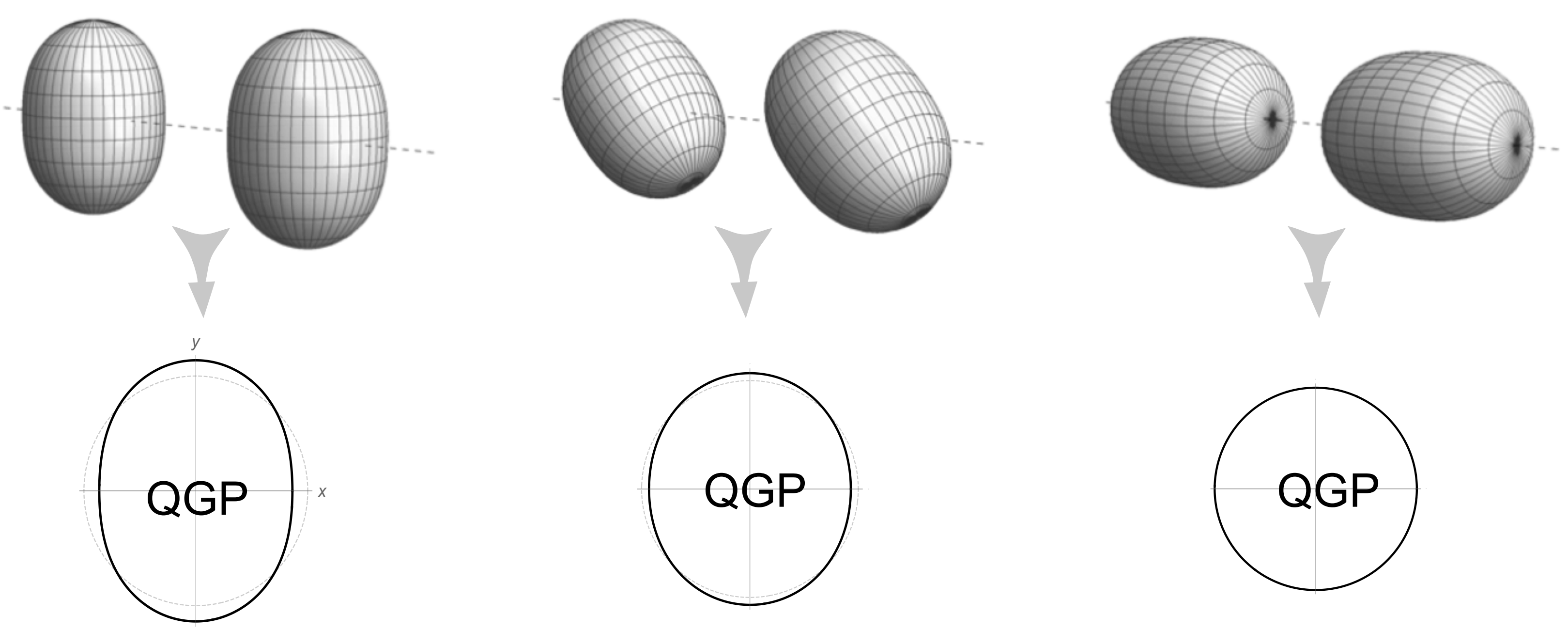

$\varepsilon_2 \sim 0.95\beta_2 \qquad \varepsilon_2 \sim 0.48\beta_2 \qquad \varepsilon_2 \sim 0$

$$\boldsymbol{\epsilon}_2 = \underbrace{\boldsymbol{\epsilon}_0}_{\text{undeformed}} + \underbrace{\boldsymbol{p}(\Omega_1,\Omega_2)}_{\text{phase factor}}\beta_2 + \mathcal{O}\left(\beta_2^2\right) \Longrightarrow \left\langle \epsilon_2^2 \right\rangle \approx \left\langle \epsilon_0^2 \right\rangle + 0.2\beta_2^2$$

Shape depends on Euler angle $\Omega = \varphi\theta\psi$

$$\left\langle v_n^2 \right\rangle \propto \left\langle \epsilon_n^2 \right\rangle$$

Intrinsic frame

Impact on high-order fluctuations

$$\rho(r,\theta,\phi) = \frac{\rho_0}{1+e^{(r-R(\theta,\phi))/a_0}} \quad R(\theta,\phi) = R_0\left(1+\beta_2[\cos\gamma Y_{2,0}+\sin\gamma Y_{2,2}]+\beta_3\sum_{m=-3}^{3}\alpha_{3,m}Y_{3,m}+\beta_4\sum_{m=-4}^{4}\alpha_{4,m}Y_{4,m}\right)$$

- In principle, can measure any moments of p(1/R, ε_2, ε_3…)
  - Mean $\langle d_\perp \rangle$ $\quad d_\perp \equiv 1/R_\perp$ $\quad \langle p_{\mathrm{T}} \rangle$
  - Variances: $\langle \varepsilon_n^2 \rangle, \left\langle (\delta d_\perp/d_\perp)^2 \right\rangle$ $\quad \langle v_n^2 \rangle, \left\langle (\delta p_{\mathrm{T}}/p_{\mathrm{T}})^2 \right\rangle$
  - Skewness $\langle \varepsilon_n^2 \delta d_\perp/d_\perp \rangle, \left\langle (\delta d_\perp/d_\perp)^3 \right\rangle$ $\quad \langle v_n^2 \delta p_{\mathrm{T}}/p_{\mathrm{T}} \rangle, \left\langle (\delta p_{\mathrm{T}}/p_{\mathrm{T}})^3 \right\rangle$
  - Kurtosis $\langle \varepsilon_n^4 \rangle - 2\langle \varepsilon_n^2 \rangle^2, \left\langle (\delta d_\perp/d_\perp)^4 \right\rangle - 3\left\langle (\delta d_\perp/d_\perp)^2 \right\rangle^2$ $\quad \langle v_n^4 \rangle - 2\langle v_n^2 \rangle^2, \left\langle (\delta p_{\mathrm{T}}/p_{\mathrm{T}})^4 \right\rangle - 3\left\langle (\delta p_{\mathrm{T}}/p_{\mathrm{T}})^2 \right\rangle^2$

    …
- All have simple connection to deformation:
  - Variances

$$\langle \varepsilon_2^2 \rangle \sim a_2 + b_2\beta_2^2$$
$$\langle \varepsilon_3^2 \rangle \sim a_3 + b_3\beta_3^2$$
$$\langle \varepsilon_4^2 \rangle \sim a_4 + b_4\beta_4^2 + b_{4,2}\beta_2^2$$
$$\left\langle (\delta d_\perp/d_\perp)^2 \right\rangle \sim a_0 + b_0\beta_2^2 + b_{0,3}\beta_3^2$$

  - Skewness

$$\left\langle \varepsilon_2^2 \delta d_\perp/d_\perp \right\rangle \sim a_1 - b_1\cos(3\gamma)\beta_2^3$$
$$\left\langle (\delta d_\perp/d_\perp)^3 \right\rangle \sim a_2 + b_2\cos(3\gamma)\beta_2^3$$

Low-energy vs high-energy method

- Intrinsic frame shape not directly visible in lab frame at time scale $\tau > I/\hbar \sim 10^{-21}s$
- Mainly inferred from non-invasive spectroscopy methods.

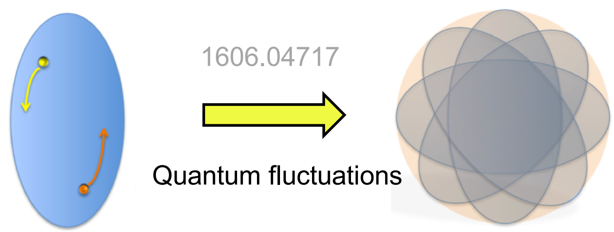

Correlated shape in intrinsic frame

Spherical shape in lab frame

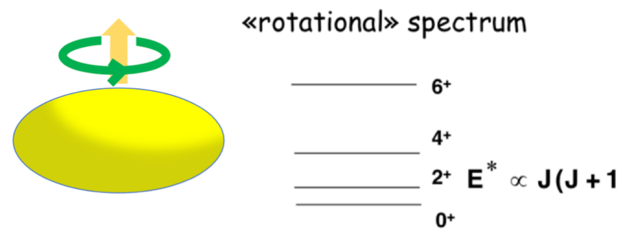

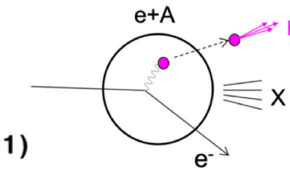

- High-energy collisions: Shape frozen in nuclear crossing (10^{-24}s << rotational time scale 10^{-21}s), probe entire mass distribution in the intrinsic frame via multi-point correlations.

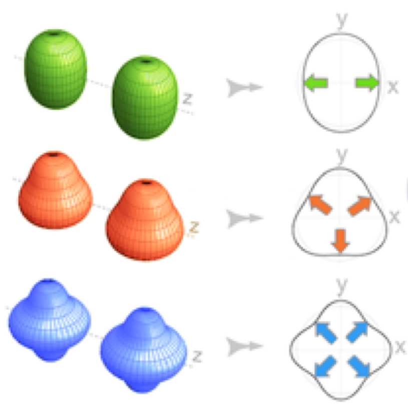

Collective flow assisted imaging

Fast crossing

$\tau \approx 2R_0/\gamma \lesssim 0.1\mathrm{fm}/c$

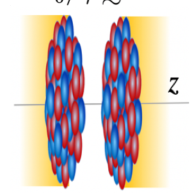

Large multiplicity

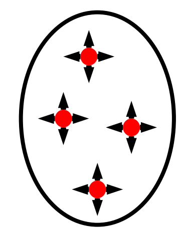

arXiv: 1902.07168

$$\mathbf{r} = re^{i\phi}$$

$$S(\mathbf{r}_1, \mathbf{r}_2) = \langle \rho(\mathbf{r}_1)\rho(\mathbf{r}_2)\rangle - \langle \rho(\mathbf{r}_1)\rangle\langle \rho(\mathbf{r}_2)\rangle$$

Intrinsic frame

$$\epsilon_2 = \frac{\int_{\mathbf{r}} \mathbf{r}^2 S(\mathbf{r})}{\int_{\mathbf{r}} |\mathbf{r}|^2 \langle S(\mathbf{r})\rangle} \Rightarrow \langle \varepsilon_2^2 \rangle = \frac{\int_{\mathbf{r}_1,\mathbf{r}_2} (\mathbf{r}_1)^2 (\mathbf{r}_2^*)^2 S(\mathbf{r}_1, \mathbf{r}_2)}{\left(\int_{\mathbf{r}} |\mathbf{r}|^2 \langle S(\mathbf{r})\rangle\right)^2}$$

Digression: Coulomb Explosion Imaging

Instantaneous stripping of electrons (thin foil or x-ray laser), and then let atoms explode under mutual coulomb repulsion

Science 244, 4903 (1989)

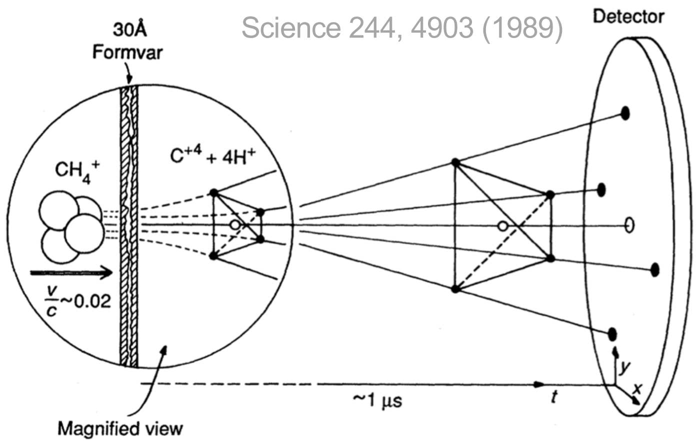

Fig. 1. A schematic view of a Coulomb explosion experiment. When a swift molecule passes through a thin solid film, it loses all of its binding electrons. The remaining positive ions repel each other, thus transforming the microstructure (as seen in the magnified view) into a macrostructure that can be measured precisely with an appropriate detector. The measured traces (x, y, t) of each fragment nucleus for individual molecules are then transformed into the original molecular structure.

Nature Physics 18, 423 (2022)

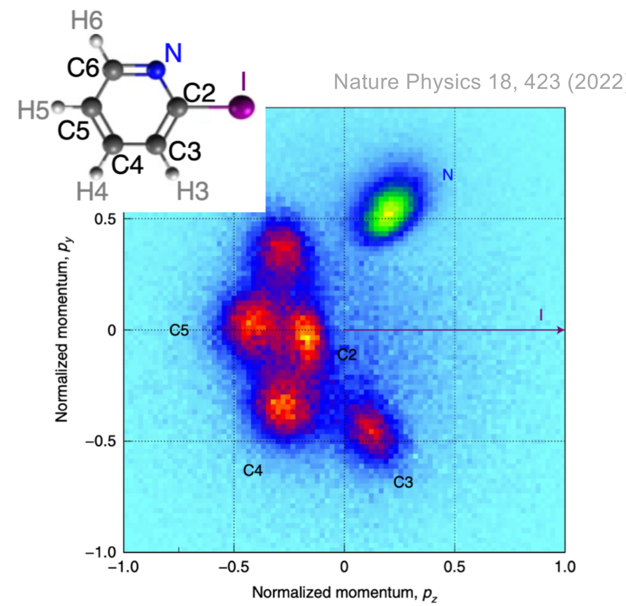

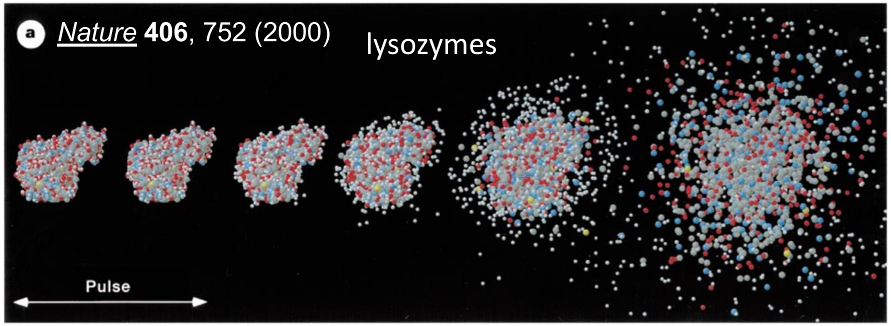

t=−2fs t=2fs t=5fs t=10fs t=−20fs t=50fs

Strategy for nuclear shape imaging

Flow observable = k ⊗ initial condition (structure)

QGP response,
a smooth function of N+Z

Structure of colliding nuclei,
non-monotonic function of N and Z

QGP

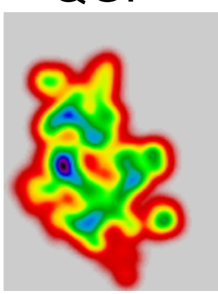

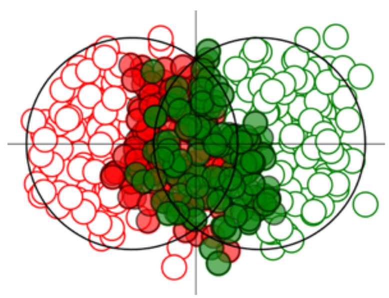

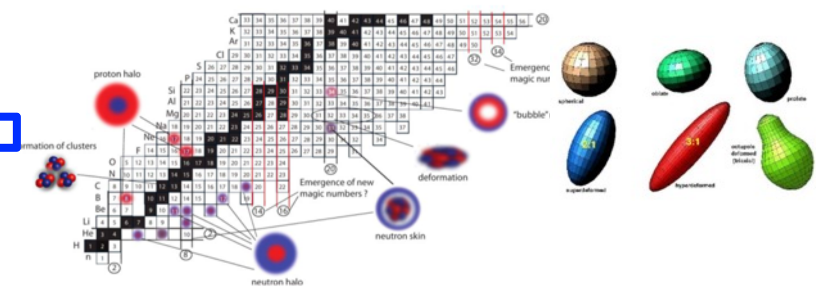

Case study: Isobar collisions at RHIC

^{96}Ru+^{96}Ru and ^{96}Zr+^{96}Zr at $\sqrt{s_{NN}}$ =200 GeV

- A key question for any HI observable O:

$$\frac{O_{^{96}\mathrm{Ru}+^{96}\mathrm{Ru}}}{O_{^{96}\mathrm{Zr}+^{96}\mathrm{Zr}}} \stackrel{?}{=} 1$$

Deviation from 1 must has origin in the nuclear structure, which impacts the initial state and then survives to the final state.

- Expectation

2109.00131

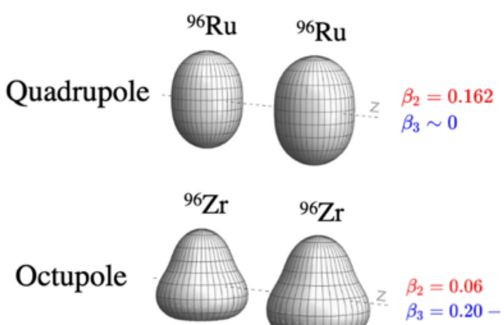

J. Jia, aXiv:2106.08768

$$\mathcal{O} \approx b_0 + b_1\beta_2^2 + b_2\beta_3^2 + b_3(R_0 - R_{0,\mathrm{ref}}) + b_4(a - a_{\mathrm{ref}})$$

$$\boxed{R_{\mathcal{O}} \equiv \frac{\mathcal{O}_{\mathrm{Ru}}}{\mathcal{O}_{\mathrm{Zr}}} \approx 1 + c_1\Delta\beta_2^2 + c_2\Delta\beta_3^2 + c_3\Delta R_0 + c_4\Delta a}$$

Species	β_2	β_3	a_0	R_0
Ru	0.162	0	0.46 fm	5.09 fm
Zr	0.06	0.20	0.52 fm	5.02 fm
difference	$\Delta\beta_2^2$	$\Delta\beta_3^2$	Δa_0	ΔR_0
	0.0226	-0.04	-0.06 fm	0.07 fm

Structure influences everywhere

$$R_{\mathcal{O}} \equiv \frac{\mathcal{O}_{\mathrm{Ru}}}{\mathcal{O}_{\mathrm{Zr}}}$$

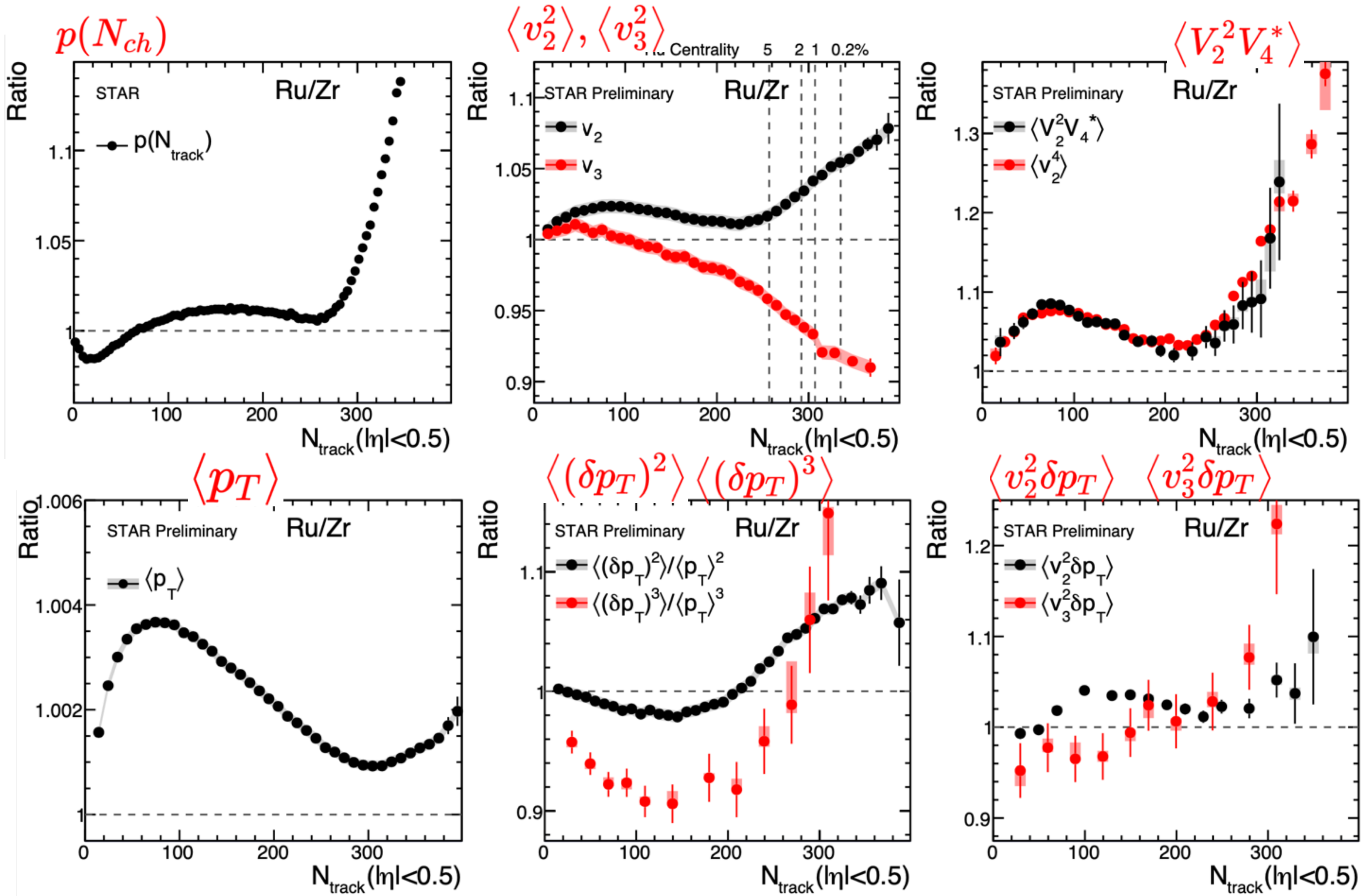

Nuclear structure via v_2-ratio and v_3-ratio

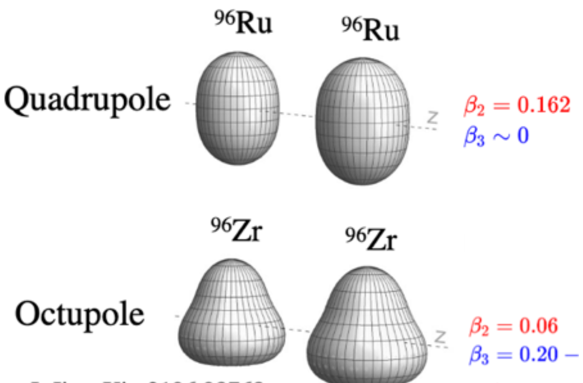

J. Jia, aXiv:2106.08768

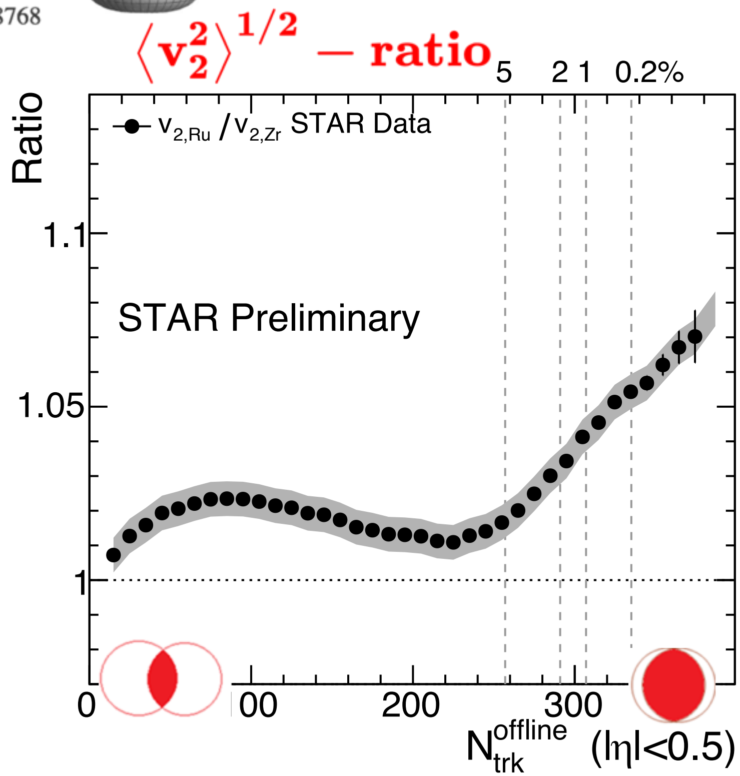

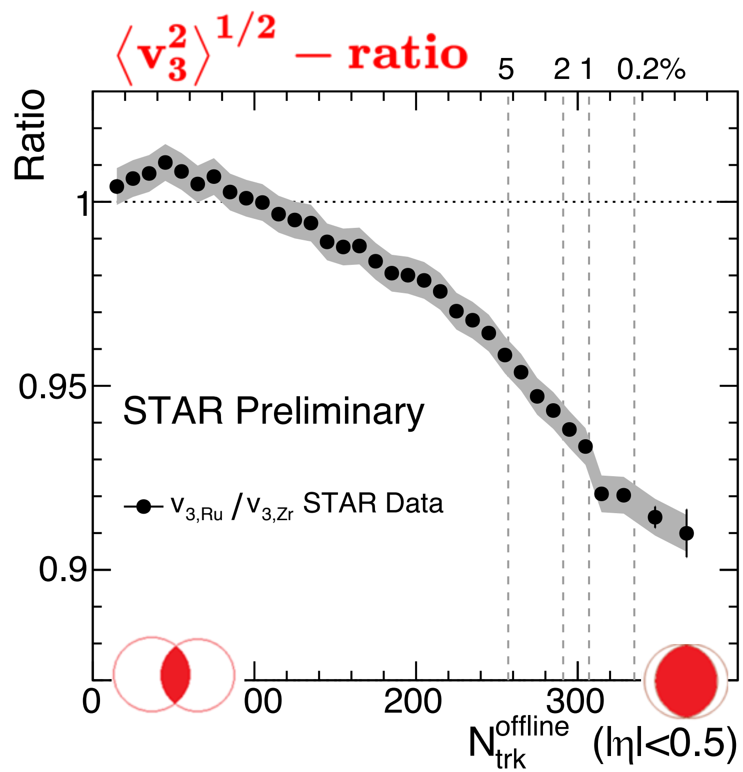

Nuclear structure via v_2-ratio and v_3-ratio

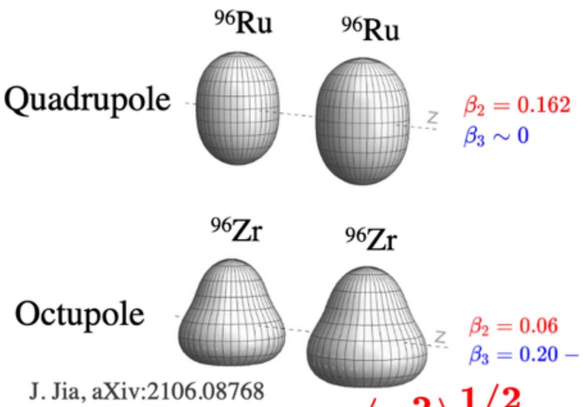

- β_{2Ru}~0.16 increase v_2, no influence on v_3 ratio
- β_{3Zr}~0.2 decrease v_2 in mid-central, decrease v_3 ratio

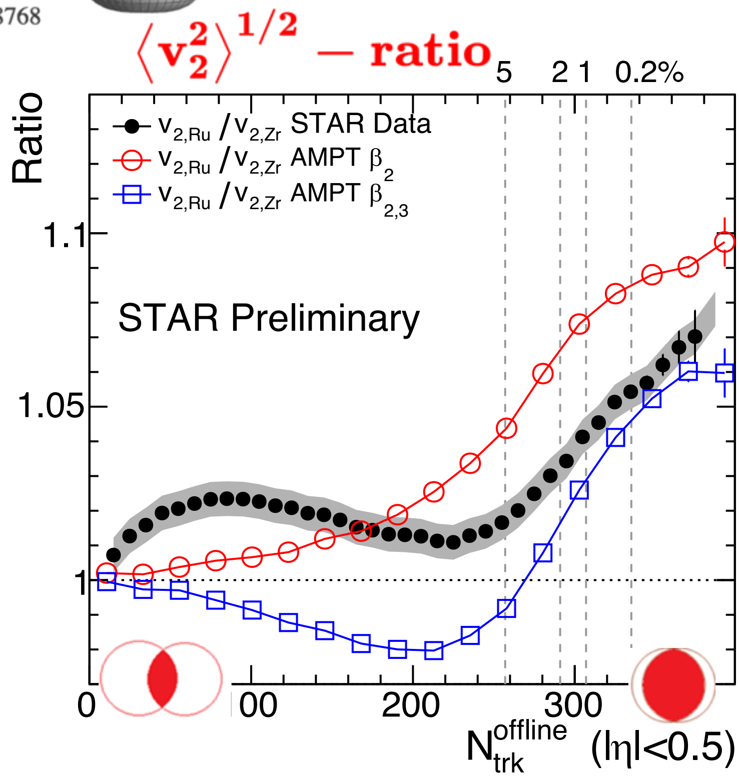

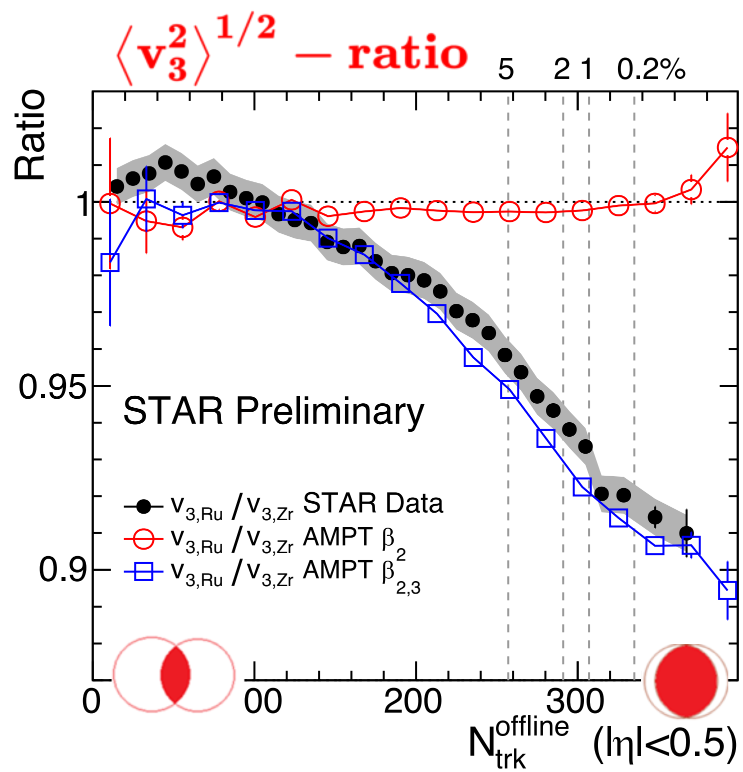

Nuclear structure via v_2-ratio and v_3-ratio

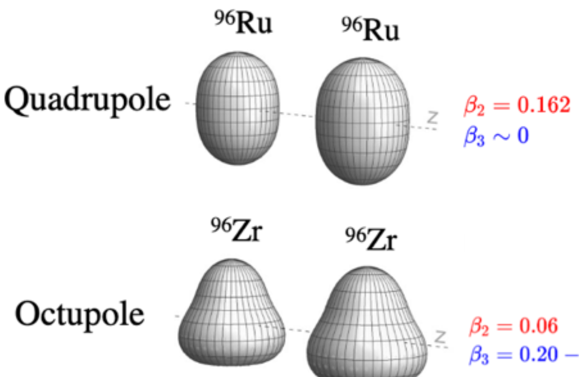

J. Jia, aXiv:2106.08768

- β_{2Ru}~0.16 increase v_2, no influence on v_3 ratio
- β_{3Zr}~0.2 decrease v_2 in mid-central, decrease v_3 ratio
- Δa_0= -0.06fm increase v_2 mid-central, small impact on v_3.
- Radius ΔR_0=0.07fm only slightly affects v_2 and v_3 ratio.

$$R_{\mathcal{O}} \equiv \frac{\mathcal{O}_{\mathrm{Ru}}}{\mathcal{O}_{\mathrm{Zr}}} \approx 1 + c_1 \Delta\beta_2^2 + c_2 \Delta\beta_3^2 + c_3 \Delta R_0 + c_4 \Delta a$$

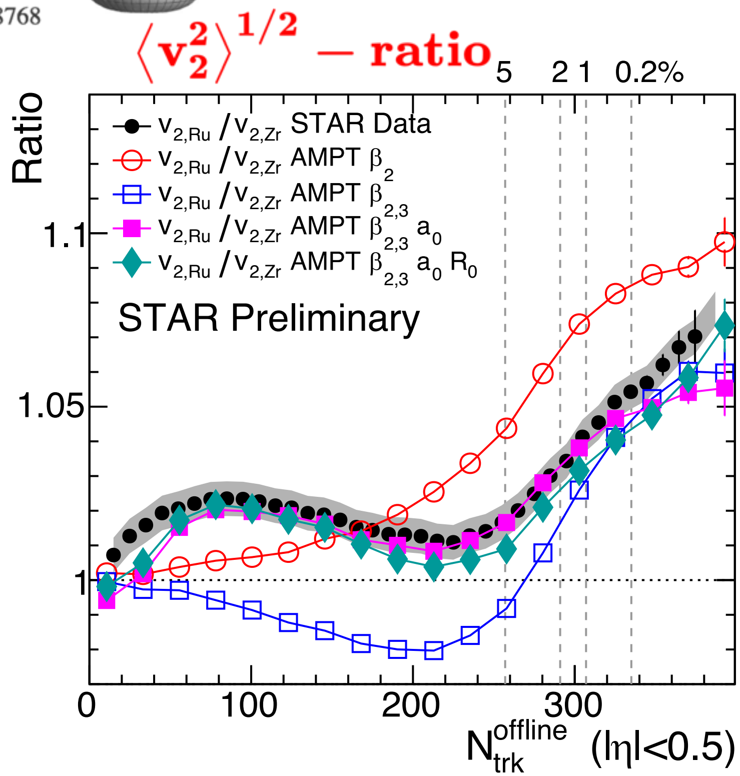

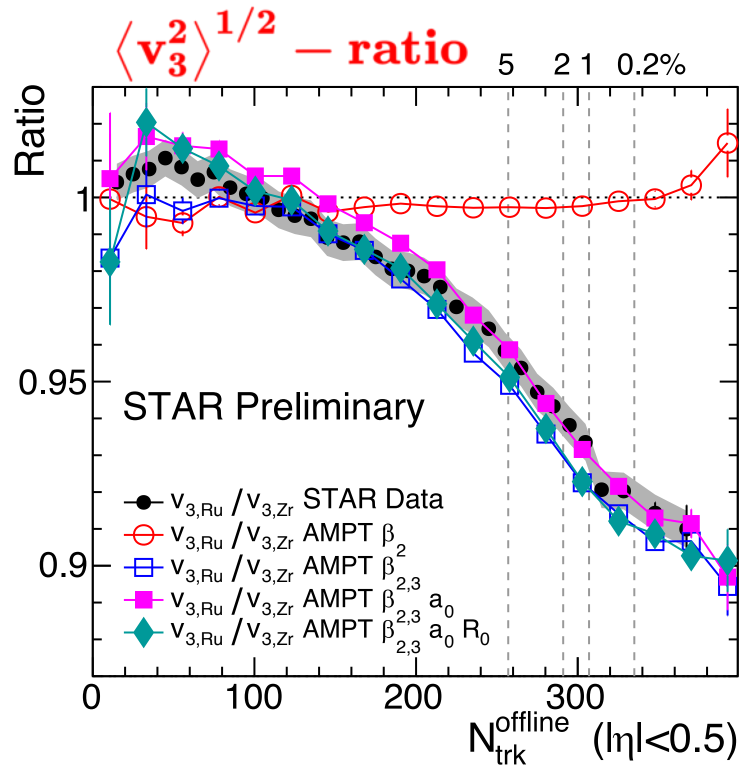

Simultaneously constrain these parameters using different N_{ch} regions

Isobar ratios cancel final state effects

- Vary the shear viscosity via partonic cross-section
  - Flow signal change by 30-50%, the v_n ratio unchanged.

$$v_n = k_n \varepsilon_n$$

$$\frac{v_{n,\mathrm{Ru}}}{v_{n,\mathrm{Zr}}} \approx \frac{\varepsilon_{n,\mathrm{Ru}}}{\varepsilon_{n,\mathrm{Zr}}}$$

Robust probe of initial state!

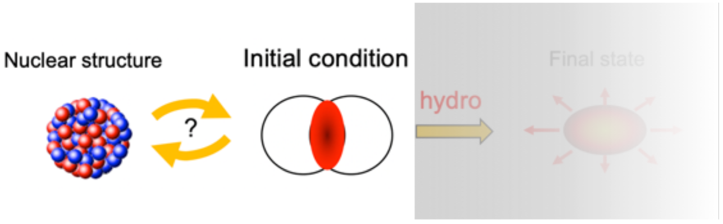

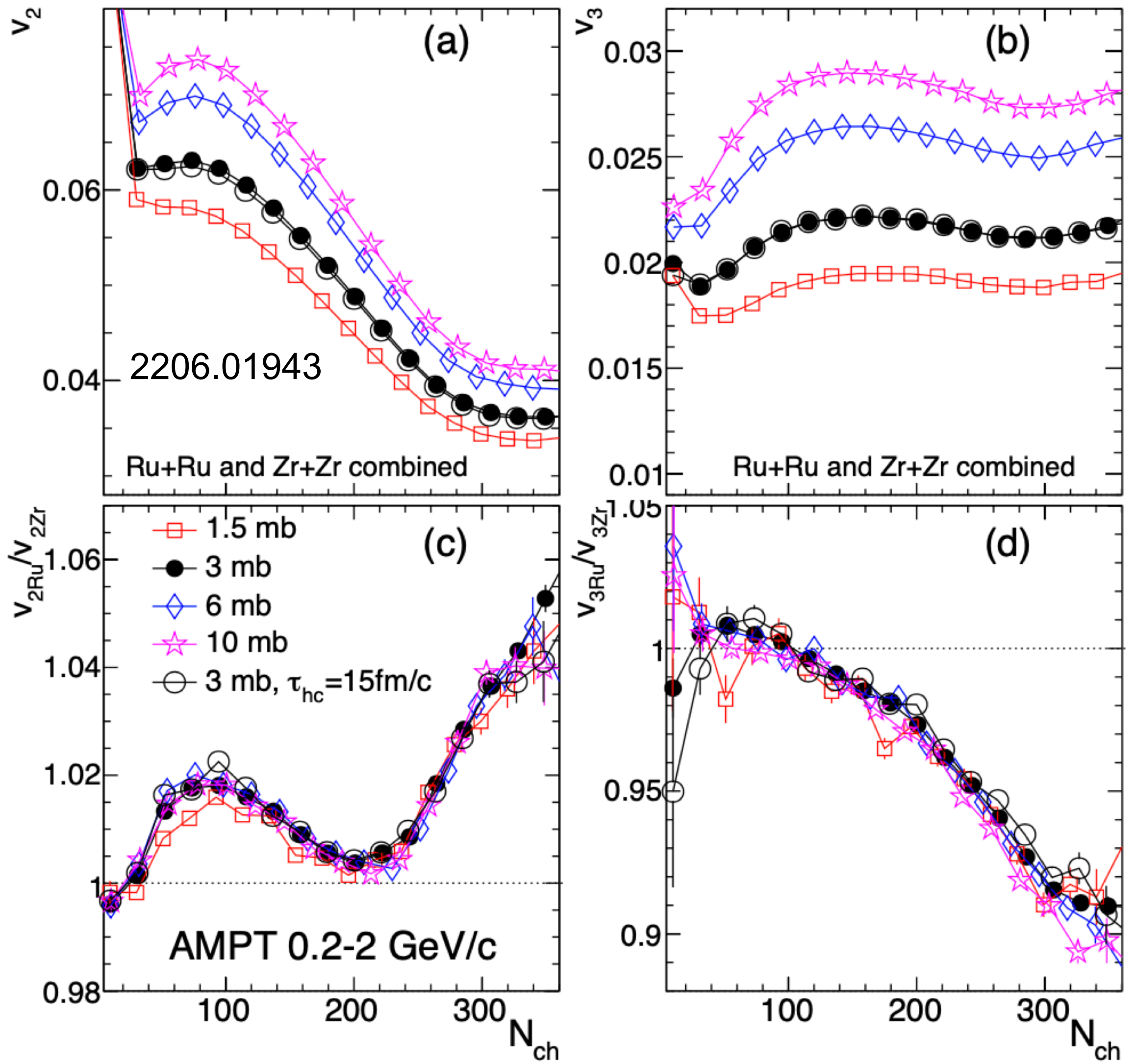

Constrain heavy-ion initial condition

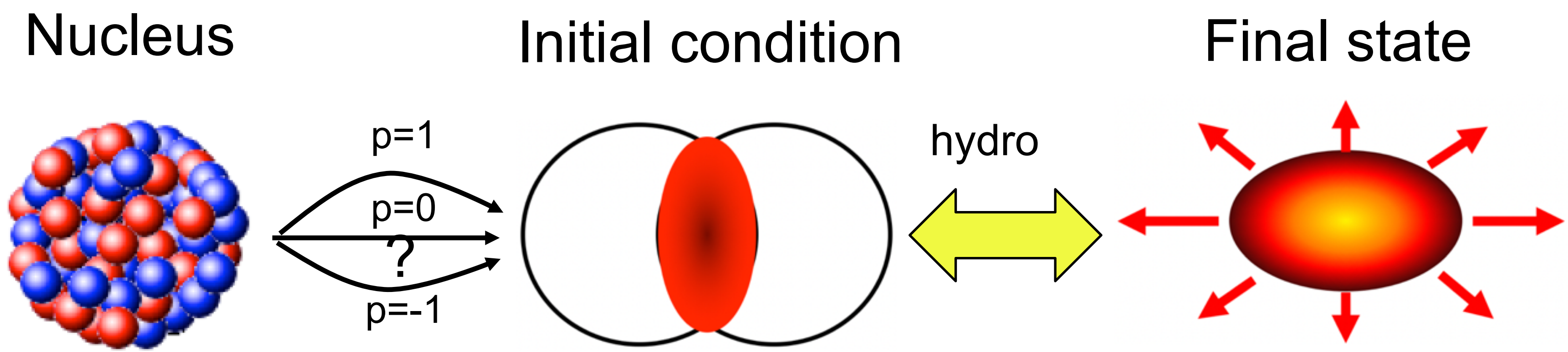

$$T_A(x,y) = \int \rho(x,y,z)dz$$

c_n relates nuclear structure and initial condition

$$\boxed{\frac{\mathcal{O}_{\mathrm{Ru}}}{\mathcal{O}_{\mathrm{Zr}}} \approx 1 + c_1\Delta\beta_2^2 + c_2\Delta\beta_3^2 + c_3\Delta R_0 + c_4\Delta a}$$

- Different ways of depositing energy $\quad T \propto \left(\frac{T_A^p + T_B^p}{2}\right)^{q/p}$

$$e(x,y) \sim \begin{cases} T_A + T_B & N_{\mathrm{part}} - \mathrm{scaling}, p = 1 \\ T_A T_B & N_{\mathrm{coll}} - \mathrm{scaling}, p = 0, q = 2 \\ \sqrt{T_A T_B} & \mathrm{Trento\ default}, p = 0 \\ \min\{T_A, T_B\} & \mathrm{KLN\ model}, p \sim -2/3 \\ T_A + T_B + \alpha T_A T_B & \mathrm{two\text{-}component\ model,} \\ & \mathrm{similar\ to\ quark\text{-}glauber\ model} \end{cases}$$

Use nuclear structure as extra lever-arm for initial condition

Triaxiality

$$R(\theta,\phi) = R_0\left(1 + \beta_2[\cos\gamma Y_{2,0} + \sin\gamma Y_{2,2}]\right.$$

1910.04673, 2004.14463

Prolate

$\beta_2 = 0.25, \cos(3\gamma) = 1$

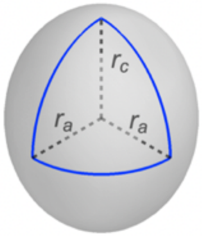

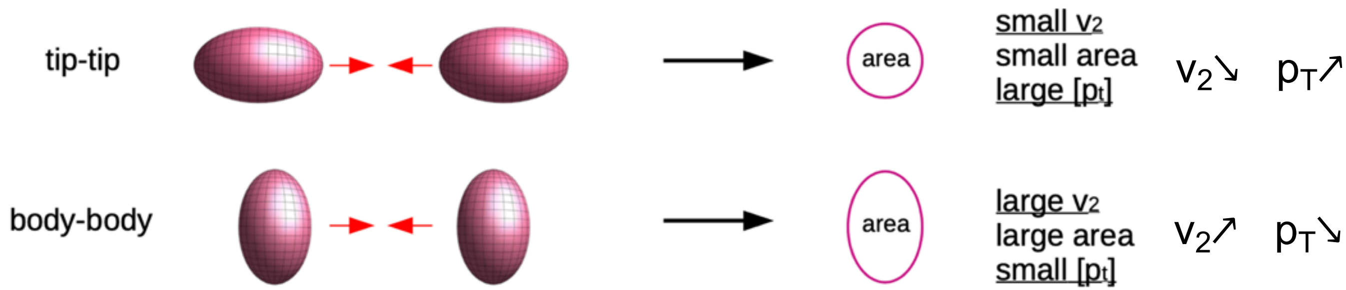

Need 3-point correlators to probe the 3 axes

$$\langle v_2^2 \delta p_T\rangle \sim -\beta_2^3\cos(3\gamma) \qquad \langle(\delta p_T)^3\rangle \sim \beta_2^3\cos(3\gamma)$$

2109.00604

Triaxial

$\beta_2 = 0.25, \cos(3\gamma) = 0$

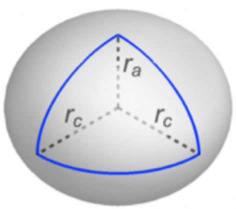

Oblate

$\beta_2 = 0.25, \cos(3\gamma) = -1$

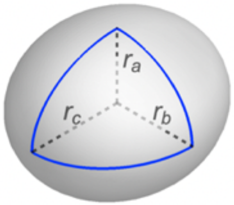

Triaxiality $R(\theta,\phi) = R_0\Big(1 + \beta_2[\cos\gamma Y_{2,0} + \sin\gamma Y_{2,2}]$

1910.04673, 2004.14463

Prolate

$\beta_2 = 0.25, \cos(3\gamma) = 1$

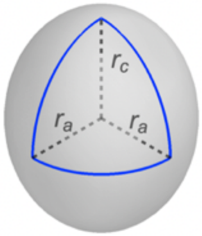

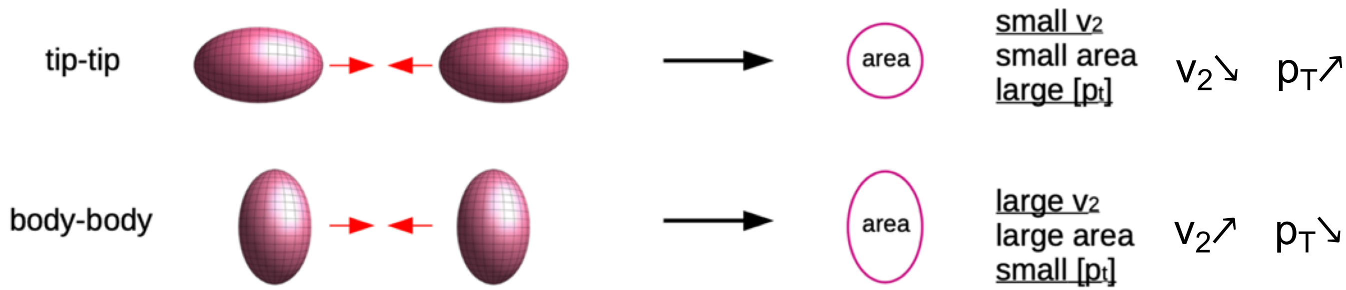

Need 3-point correlators to probe the 3 axes

$$\langle v_2^2 \delta p_T\rangle \sim -\beta_2^3\cos(3\gamma) \qquad \langle(\delta p_T)^3\rangle \sim \beta_2^3\cos(3\gamma)$$

2109.00604

Triaxial

$\beta_2 = 0.25, \cos(3\gamma) = 0$

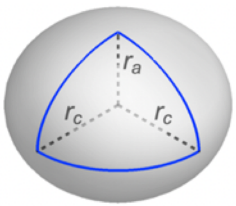

Oblate

$\beta_2 = 0.25, \cos(3\gamma) = -1$

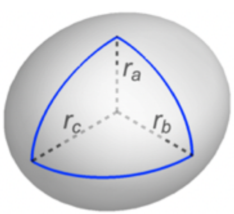

Compare U+U vs Au+Au: β_{2U} ~ 0.28, β_{2Au}~ 0.13:

v_2-$[p_T]$ covariance

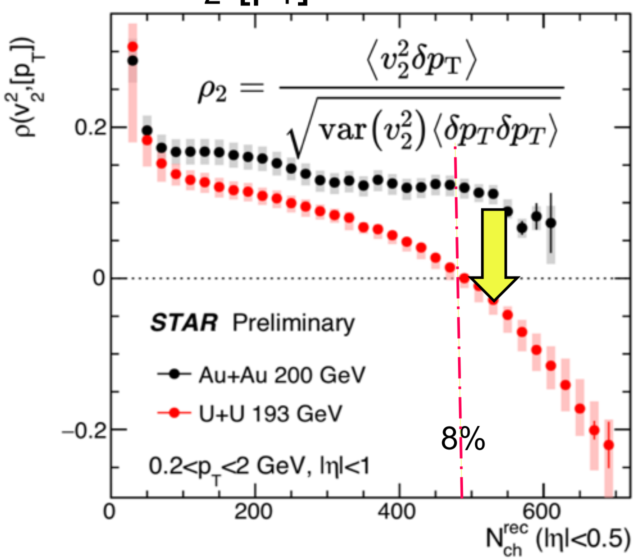

$[p_T]$ skewness

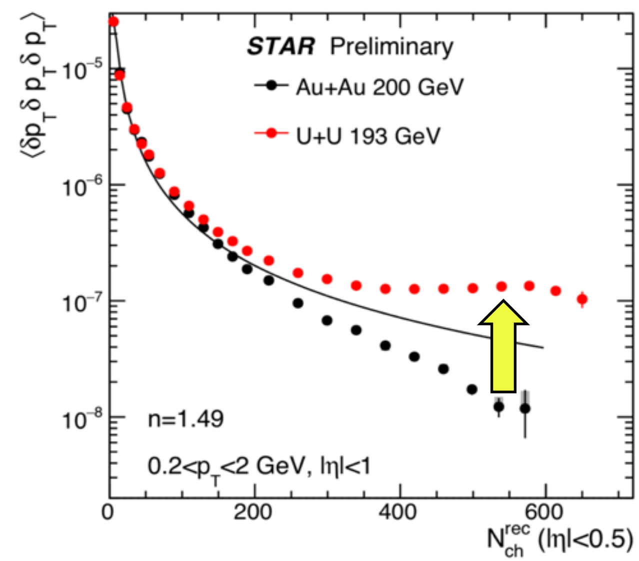

Opportunities at the intersection of nuclear structure and hot QCD

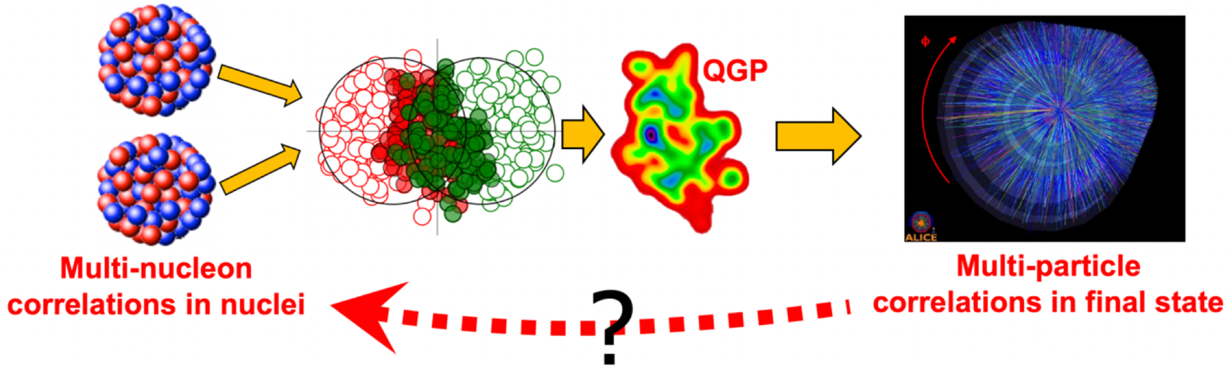

Many examples in https://arxiv.org/abs/2209.11042, but here is my list

- Probe octupole and hexadecapole deformations via v3 and v4 in central collisions.
- Gauge shape of odd-mass nuclei by comparing with neighboring even-even nuclei.
- Separate average shape from shape fluctuations via multi-particle correlations
- Constrain the radial structure of nuclei, including the neutron skin
- Structure in small systems including alpha clustering (e.g. $^{16}O+^{16}O$ vs $^{20}Ne+^{20}Ne$)

……

See recent INT program 23-1A

Shape evolution of $^{144-154}$Sm isotopic chain

Transition from nearly-spherical to well-deformed nuclei when size increase by less than 7%. Using HI to access the multi-nucleon correlations leading to such shape evolution, as well as dynamical β_3 and β_4 shape fluctuations (in addition to initial condition)

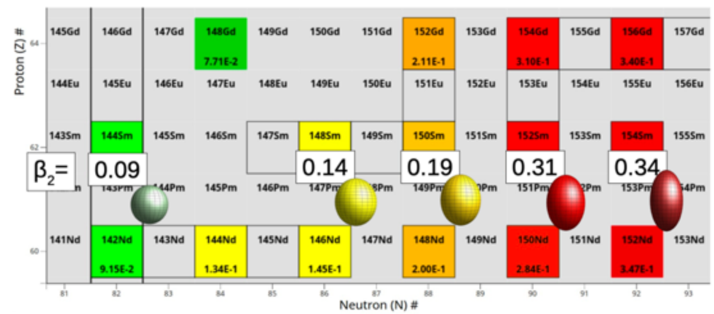

In central collisions

$$\langle \epsilon_2^2 \rangle = a' + b'\beta_2^2 \qquad a' = \langle \varepsilon_2^2 \rangle_{|\beta_2=0} \propto 1/A$$

$$\langle v_2^2 \rangle = a + b\beta_2^2 \qquad a = \langle v_2^2 \rangle_{|\beta_2=0} \propto 1/A$$

b', b are ~ independent of system

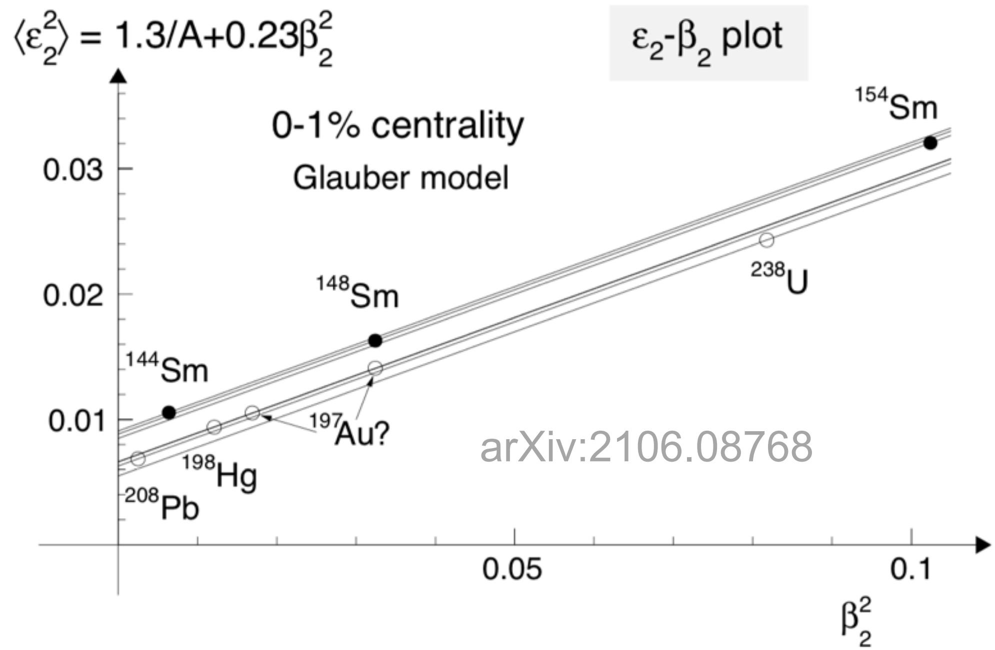

Systems with similar A falls on the same curve.

Fix a and b with two isobar systems with known β_2, then predict others.

Influence of triaxiality: Glauber model

Skewness sensitive to γ

Described by

$$\left\langle \varepsilon_2^2 \frac{\delta d_\perp}{d_\perp} \right\rangle \propto \langle v_2^2 \delta p_\mathrm{T} \rangle \propto a + b\cos(3\gamma)\beta_2^3$$

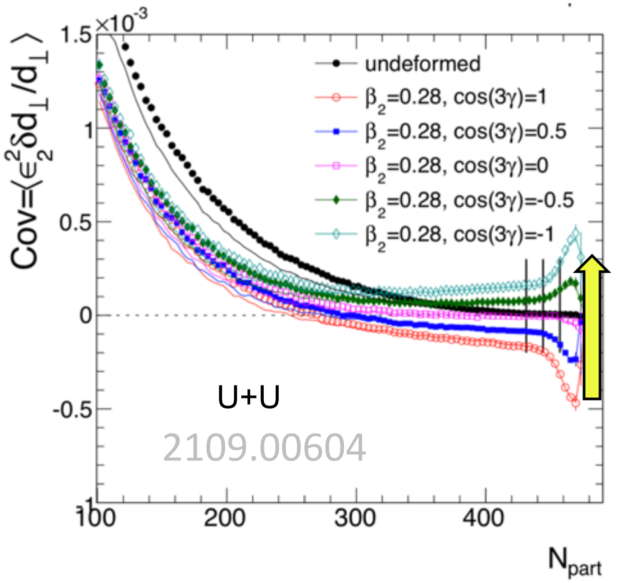

variances insensitive to γ

$$\langle \varepsilon_2^2 \rangle \propto \langle v_2^2 \rangle \propto a + b\beta_2^2$$

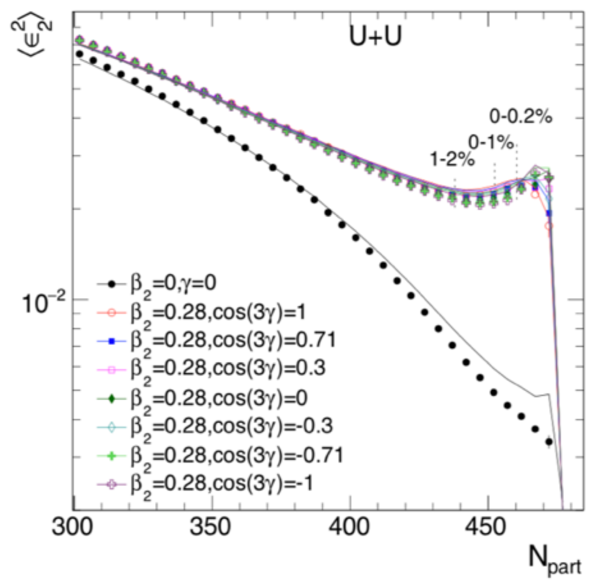

Use variance to constrain β_2, use skewness to constrain γ

(β_2,γ) diagram in heavy-ion collisions

The (β_2,γ) dependence in 0-1% U+U Glauber model can be approximated by:

$$d_\perp \propto 1/R_\perp$$

$$\langle \varepsilon_2^2 \rangle \approx [0.02 + \beta_2^2] \times 0.235$$

$$\langle (\delta d_\perp/d_\perp)^2 \rangle \approx [0.035 + \beta_2^2] \times 0.0093$$

$$\langle \varepsilon_2^2 \delta d_\perp/d_\perp \rangle \approx [0.0005 - (0.07 + 1.36\cos(3\gamma))\beta_2^3] \times 10^{-2}$$

$$\rho = \frac{\langle \varepsilon_2^2 \delta d_\perp \rangle}{\langle \varepsilon_2^2 \rangle \sqrt{\langle (\delta d_\perp)^2 \rangle}}$$

Map from (β_2,γ) plane to HI observables

How about $\langle v_2^2 \delta[p_T] \rangle$ vs. $\langle v_2^2 \rangle$

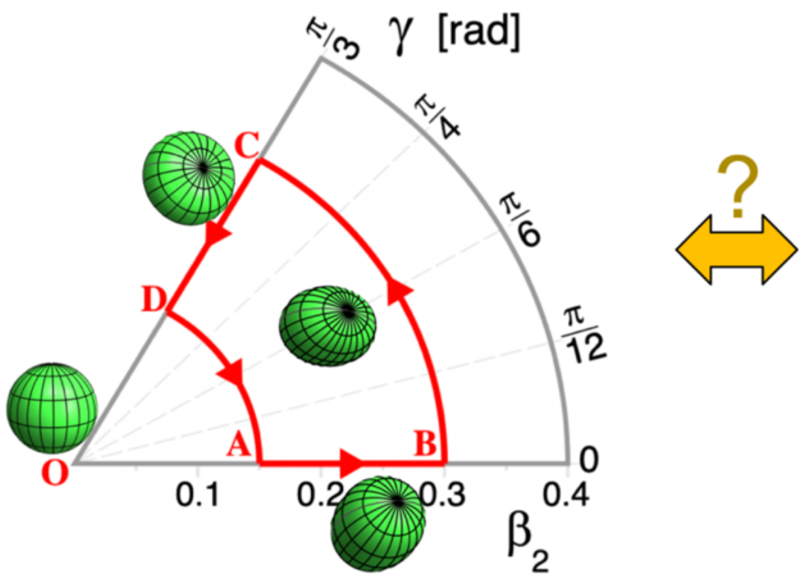

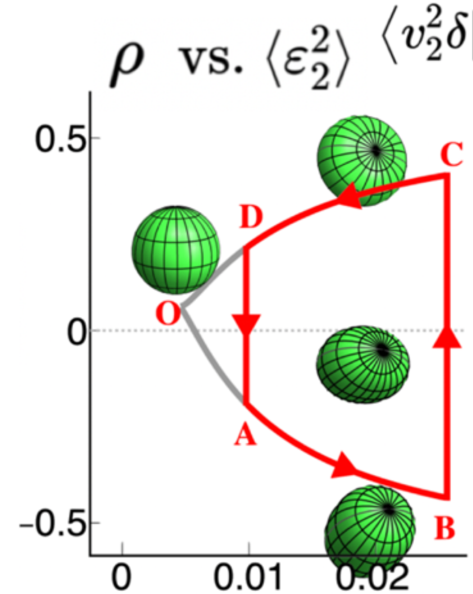

Collision system scan to map out this trajectory: calibrate coefficients with species with known β,γ, then predict for species of interest.

Effect of shape fluctuations

$$\boxed{\rho_{2,\mathrm{Xe}}^{\mathrm{pcc}}/\rho_{2,\mathrm{Pb}}^{\mathrm{pcc}}} \qquad \rho_2^{\mathrm{pcc}} \equiv \frac{\langle v_2^2 \delta p_{\mathrm{T}}\rangle}{\sqrt{\mathrm{var}(v_2^2)}\sqrt{\langle(\delta p_{\mathrm{T}})^2\rangle}}$$

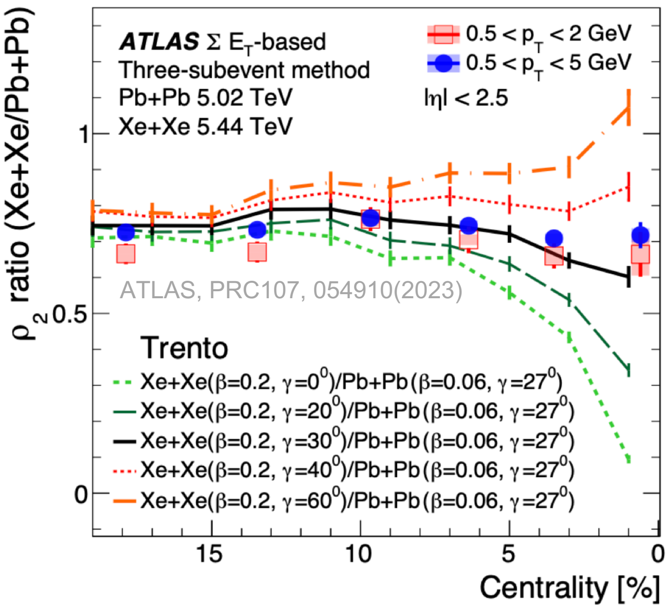

$$\langle\cos(3\gamma)\rangle \approx \exp\left(-9\sigma_\gamma^2/2\right)\cos(3\bar{\gamma})$$

$$\sigma_\gamma^2 = \langle(\gamma-\bar{\gamma})^2\rangle$$

2301.03556

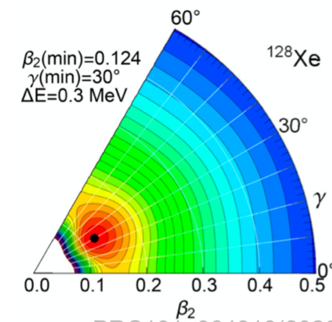

PRC101, 064318(2020)

Fluctuation in γ damps difference between prolate and oblate, such that all results approach triaxial case

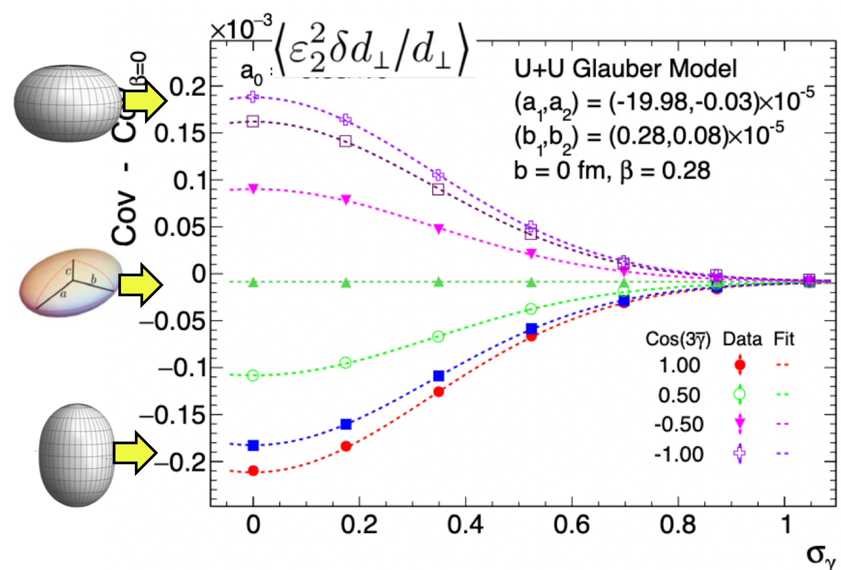

Ratio support average triaxial shape of [129]Xe
But only if $\boldsymbol{\beta}_{2\mathrm{Xe}}$ is large and fluctuation of $\boldsymbol{\gamma}_{\mathrm{Xe}}$ small

$$\langle v_2^2 \delta p_{\mathrm{T}}\rangle \approx a - b\langle \beta_2^3 \cos(3\gamma)\rangle$$

Separate average shape and its fluctuations

- Shape fluctuations and shape coexistence can be accessed via high-order correlations.

Shape coexistence

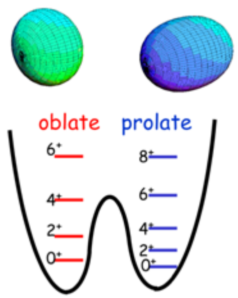

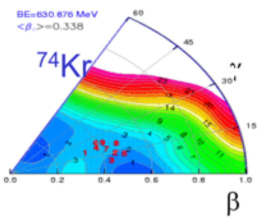

quadrupole operator $\hat{Q}$

$$\begin{cases} \langle\beta^2\rangle = \dfrac{16\pi^2}{9A^2R_0^4}\left\langle\hat{Q}^2\right\rangle & \text{2-p correlation} \\ \sigma^2(\langle\beta^2\rangle)/\langle\beta^2\rangle = \sigma^2\left(\langle\hat{Q}^2\rangle\right)/\langle\hat{Q}^2\rangle & \text{4-p correlation} \end{cases}$$

1906.07542

$$\begin{cases} \langle\cos 3\gamma\rangle = -\sqrt{\dfrac{7}{2}}\dfrac{\left\langle\hat{Q}^3\right\rangle}{\left\langle\hat{Q}^2\right\rangle^{3/2}} & \text{3-p correlation} \\ \dfrac{\sigma^2(\cos 3\gamma)}{(\cos 3\gamma)^2} = \dfrac{\sigma^2\langle\hat{Q}^3\rangle}{\langle\hat{Q}^3\rangle^2} + \dfrac{9}{4}\dfrac{\sigma^2\langle\hat{Q}^2\rangle}{\langle\hat{Q}^2\rangle^2} - 3\dfrac{\langle\hat{Q}^5\rangle - \langle\hat{Q}^3\rangle\langle\hat{Q}^2\rangle}{\langle\hat{Q}^3\rangle\langle\hat{Q}^2\rangle} & \text{6-p correlation} \end{cases}$$

Heavy ion observables:

arXiv:2301.03556

$$\frac{\left\langle\varepsilon_2^2\right\rangle}{\frac{3}{4\pi}\left\langle\beta_2^2\right\rangle} \Longleftrightarrow \frac{\left\langle\varepsilon_2^4\right\rangle - 2\left\langle\varepsilon_2^2\right\rangle^2}{-\frac{9}{112\pi^2}\left(7\left\langle\beta_2^2\right\rangle^2 - 5\left\langle\beta_2^4\right\rangle\right)}$$

$$\frac{\left\langle\varepsilon_2^2(\delta d_\perp/d_\perp)\right\rangle}{-\frac{3\sqrt{5}}{112\pi^{3/2}}\left\langle\cos(3\gamma)\beta_2^3\right\rangle} \Longleftrightarrow \frac{\left(\left\langle\varepsilon_2^6\right\rangle - 9\left\langle\varepsilon_2^4\right\rangle\left\langle\varepsilon_2^2\right\rangle + 12\left\langle\varepsilon_2^2\right\rangle^3\right)/4}{\frac{81}{256\pi^3}\left[\left\langle\beta_2^2\right\rangle^3 - \frac{45}{14}\left\langle\beta_2^4\right\rangle\left\langle\beta_2^2\right\rangle - \frac{1175}{6006}\left\langle\beta_2^6\right\rangle + \frac{25}{3003}\left\langle\cos(6\gamma)\beta_2^6\right\rangle\right]}$$

Sensitivity to the radial structure

$$\boxed{R_{\mathcal{O}} \equiv \frac{\mathcal{O}_{\mathrm{Ru}}}{\mathcal{O}_{\mathrm{Zr}}} \approx 1 + c_1 \Delta\beta_2^2 + c_2 \Delta\beta_3^2 + c_3 \Delta R_0 + c_4 \Delta a}$$

Relate to neutron skin: $\Delta r_{\mathrm{np}} = \langle r_n \rangle^{1/2} - \langle r_p \rangle^{1/2}$

$$\Delta r_{np,\mathrm{Ru}} - \Delta r_{np,\mathrm{Zr}} \propto (R_0 \Delta R_0 - R_{0p} \Delta R_{0p}) + 7/3\pi^2 (a \Delta a - a_p \Delta a_p)$$

charge

mass

Sensitivity to radial structure

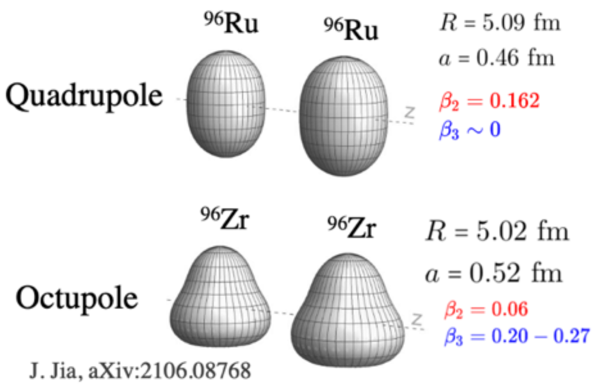

- For N_{ch} ratio:
  - β_{2Ru}~0.16 decrease ratio, increase after considering β_{3Zr}~0.2
  - The bump structure in non-central region from Δa_0 and ΔR_0
- For $\langle p_T \rangle$ ratio:
  - Strong influence from Δa_0 and ΔR_0

$$R_{\mathcal{O}} \equiv \frac{\mathcal{O}_{\rm Ru}}{\mathcal{O}_{\rm Zr}} \approx 1 + c_1 \Delta\beta_2^2 + c_2 \Delta\beta_3^2 + c_3 \Delta R_0 + c_4 \Delta a$$

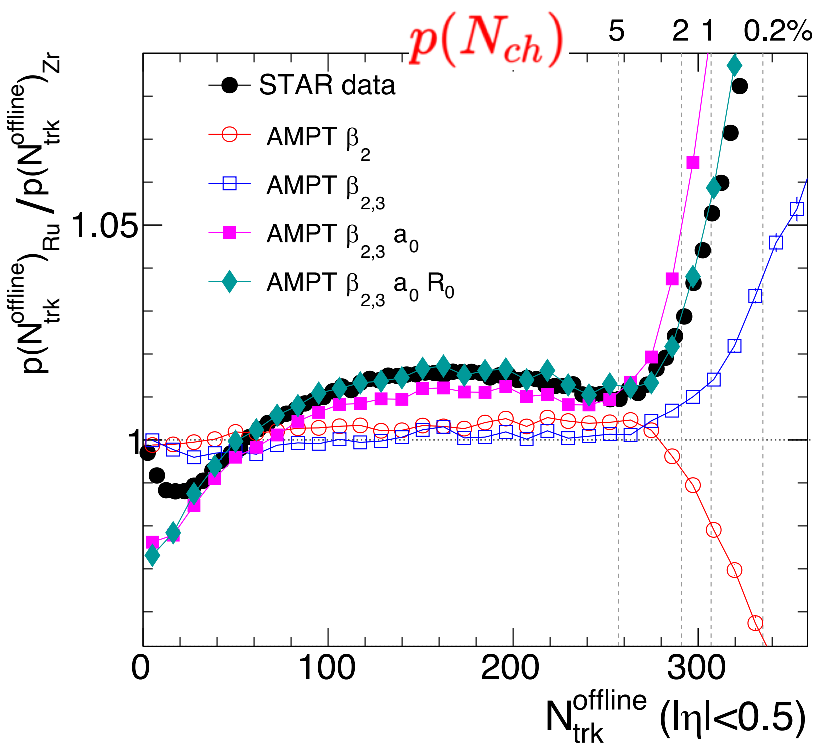

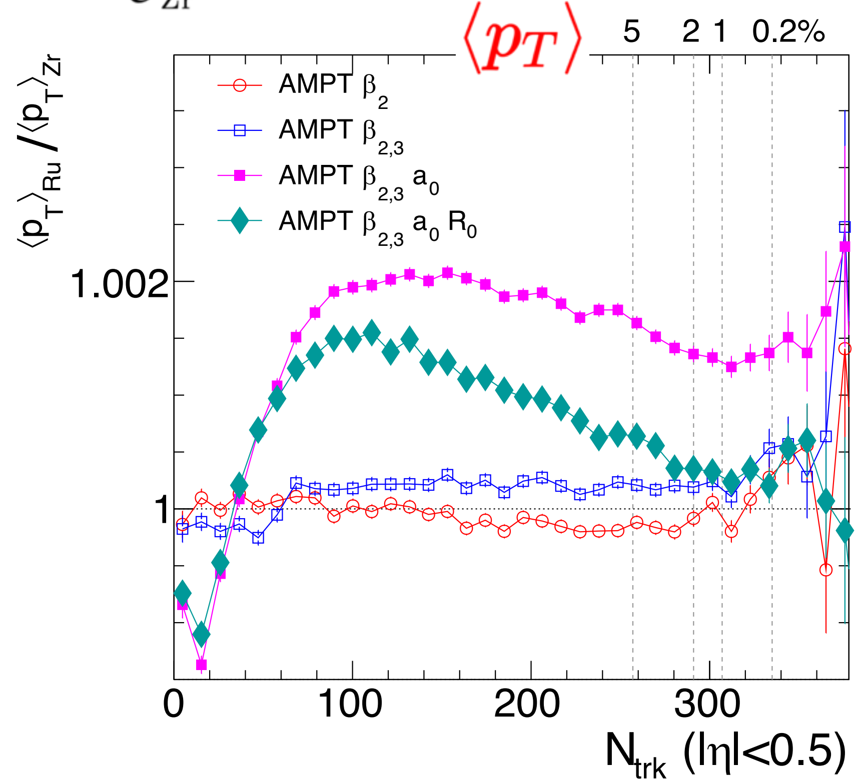

Δa_0 and ΔR_0 influences add up

Δa_0 and ΔR_0 influences partially cancel

Separating shape and size effects

Nuclear skin contributes to $v_2^{rp} \sim v_2\{4\}$, deformation contribute to fluctuations

$$\langle v_2^2 \rangle = \underbrace{\left(v_2^{\mathrm{rp}}\right)^2}_{\text{mean}} + \underbrace{\delta^2}_{\text{fluctuations}}$$

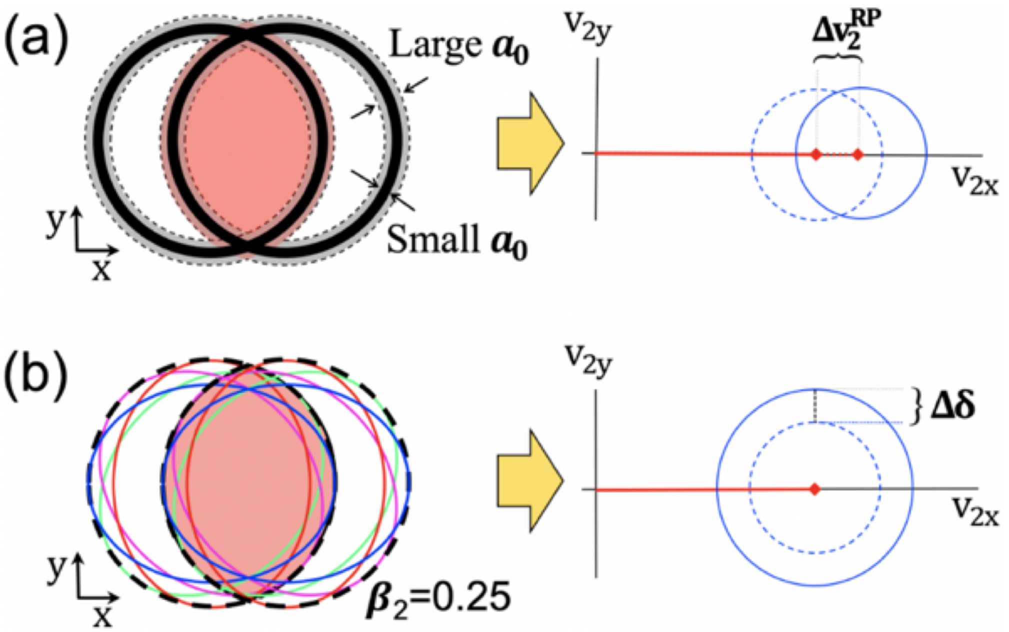

Separating shape and size effects

Nuclear skin contributes to $v_2^{rp} \sim v_2\{4\}$, deformation contribute to fluctuations

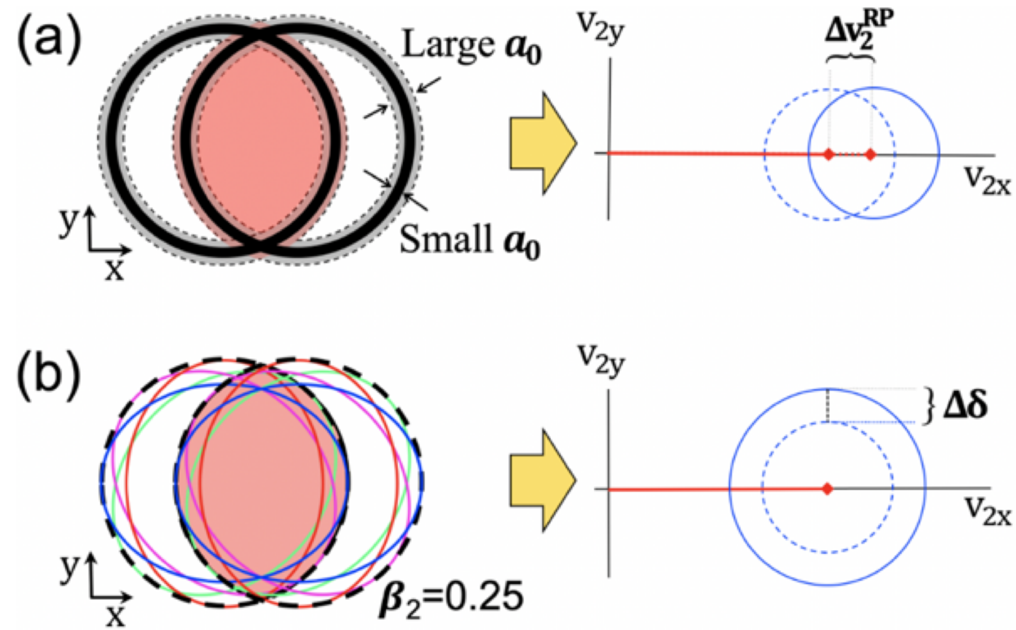

$$\langle v_2^2 \rangle = \underbrace{(v_2^{\mathrm{rp}})^2}_{\text{mean}} + \underbrace{\delta^2}_{\text{fluctuations}}$$

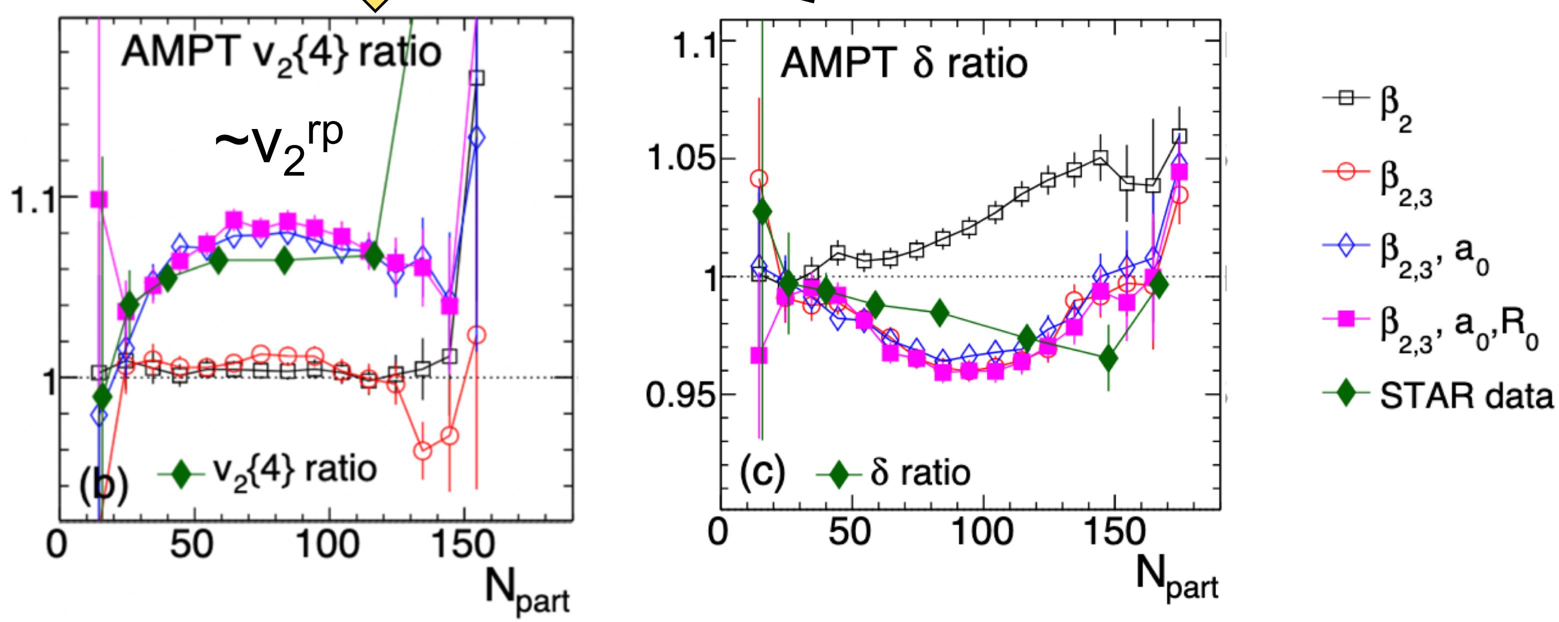

Neutron skin in high-energy collisions

PREX and CREX has tension with theory and previous exp. Indicate a larger L value.

$$\Delta r_{\mathrm{np,Pb}} = 0.28 \pm 0.07\mathrm{fm}$$
$$\Delta r_{\mathrm{np,Ca}} = 0.14 \pm 0.03\mathrm{fm}$$

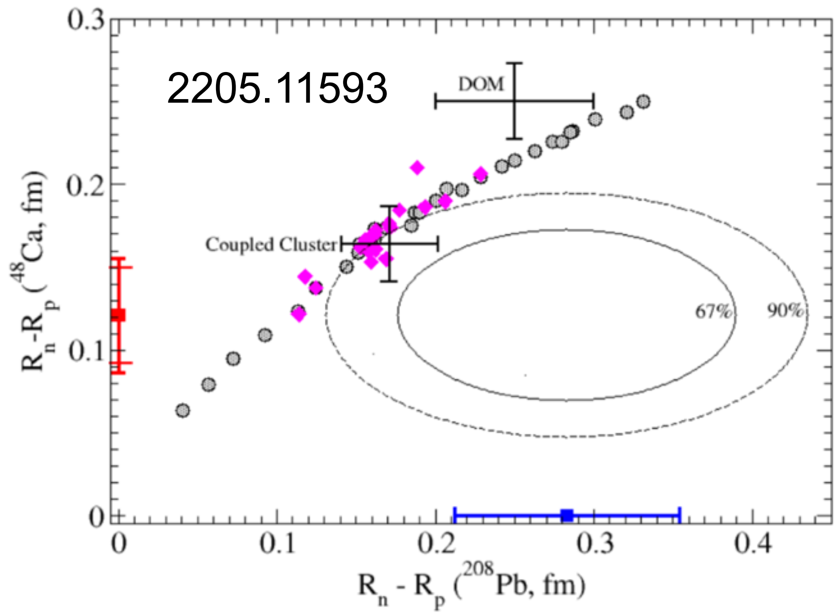

- Access the difference of neutron skin by comparing 40Ca+40Ca and 48Ca+48Ca

We know:
$$\sqrt{\langle r_{\mathrm{p}}^2\rangle}(^{48}\mathrm{Ca}) = \sqrt{\langle r_{\mathrm{p}}^2\rangle}(^{40}\mathrm{Ca})$$
$$\sqrt{\langle r_{\mathrm{p}}^2\rangle}(^{40}\mathrm{Ca}) \approx \sqrt{\langle r_{\mathrm{n}}^2\rangle}(^{40}\mathrm{Ca})$$

Hence :
$$\Delta_{\mathrm{np}}(^{48}\mathrm{Ca}) - \Delta_{\mathrm{np}}(^{40}\mathrm{Ca}) \simeq \Delta_{\mathrm{np}}(^{48}\mathrm{Ca})$$
$$\propto \bar{R}_0 \Delta R_0 + 7/3\pi^2 \bar{a}\Delta a$$

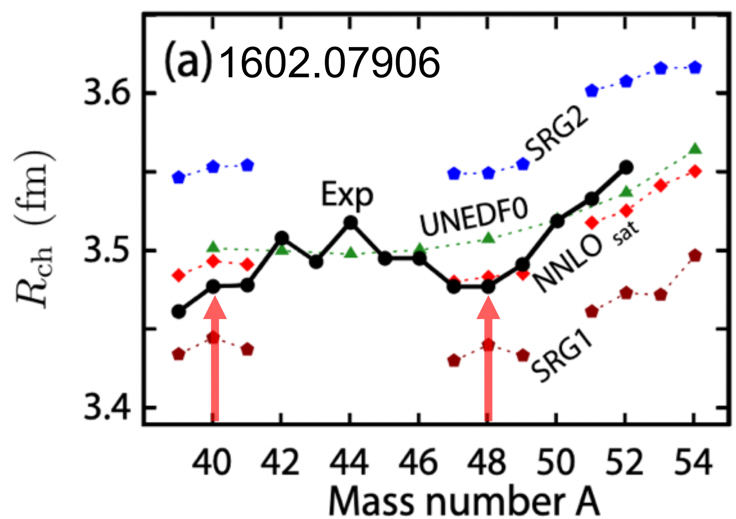

Summary and outlook

- High-energy collisions image nuclear shape at ultra-short time scale of 10^{-24}s; Large particle multiplicity enables many-particle correlation event-by-event to probe many-nucleon correlations in nuclei (relatively more challenging to measure in low energy).

- Collisions of carefully-selected isobar species (at LHC) can reveal the many-body nucleon correlations & constrain the heavy ion initial condition from small to large nuclei

A	isobars	A	isobars	A	isobars	A	isobars	A	isobars	A	isobars
36	Ar, S	80	Se, Kr	106	Pd, Cd	124	Sn, Te, Xe	148	Nd, Sm	174	Yb, Hf
40	Ca, Ar	84	Kr, Sr, Mo	108	Pd, Cd	126	Te, Xe	150	Nd, Sm	176	Yb, Lu, Hf
46	Ca, Ti	86	Kr, Sr	110	Pd, Cd	128	Te, Xe	152	Sm, Gd	180	Hf, W
48	Ca, Ti	87	Rb, Sr	112	Cd, Sn	130	Te, Xe, Ba	154	Sm, Gd	184	W, Os
50	Ti, V, Cr	92	Zr, Nb, Mo	113	Cd, In	132	Xe, Ba	156	Gd,Dy	186	W, Os
54	Cr, Fe	94	Zr, Mo	114	Cd, Sn	134	Xe, Ba	158	Gd,Dy	187	Re, Os
64	Ni, Zn	96	Zr, Mo, Ru	115	In, Sn	136	Xe, Ba, Ce	160	Gd,Dy	190	Os, Pt
70	Zn, Ge	98	Mo, Ru	116	Cd, Sn	138	Ba, La, Ce	162	Dy,Er	192	Os, Pt
74	Ge, Se	100	Mo, Ru	120	Sn, Te	142	Ce, Nd	164	Dy,Er	196	Pt, Hg
76	Ge, Se	102	Ru, Pd	122	Sn, Te	144	Nd, Sm	168	Er,Yb	198	Pt, Hg
78	Se, Kr	104	Ru, Pd	123	Sb, Te	146	Nd, Sm	170	Er,Yb	204	Hg, Pb

arXiv:2102.08158

TABLE I. Pairs and triplets of stable isobars (half-life $> 10^8$ y). 141 nuclides are listed. The region marked in red contains large strongly-deformed nuclei ($\beta_2 > 0.2$). The region marked in blue corresponds to nuclides which may present an octupole deformation in their ground state [48].

Build multi-particle correlators (moments) over these events

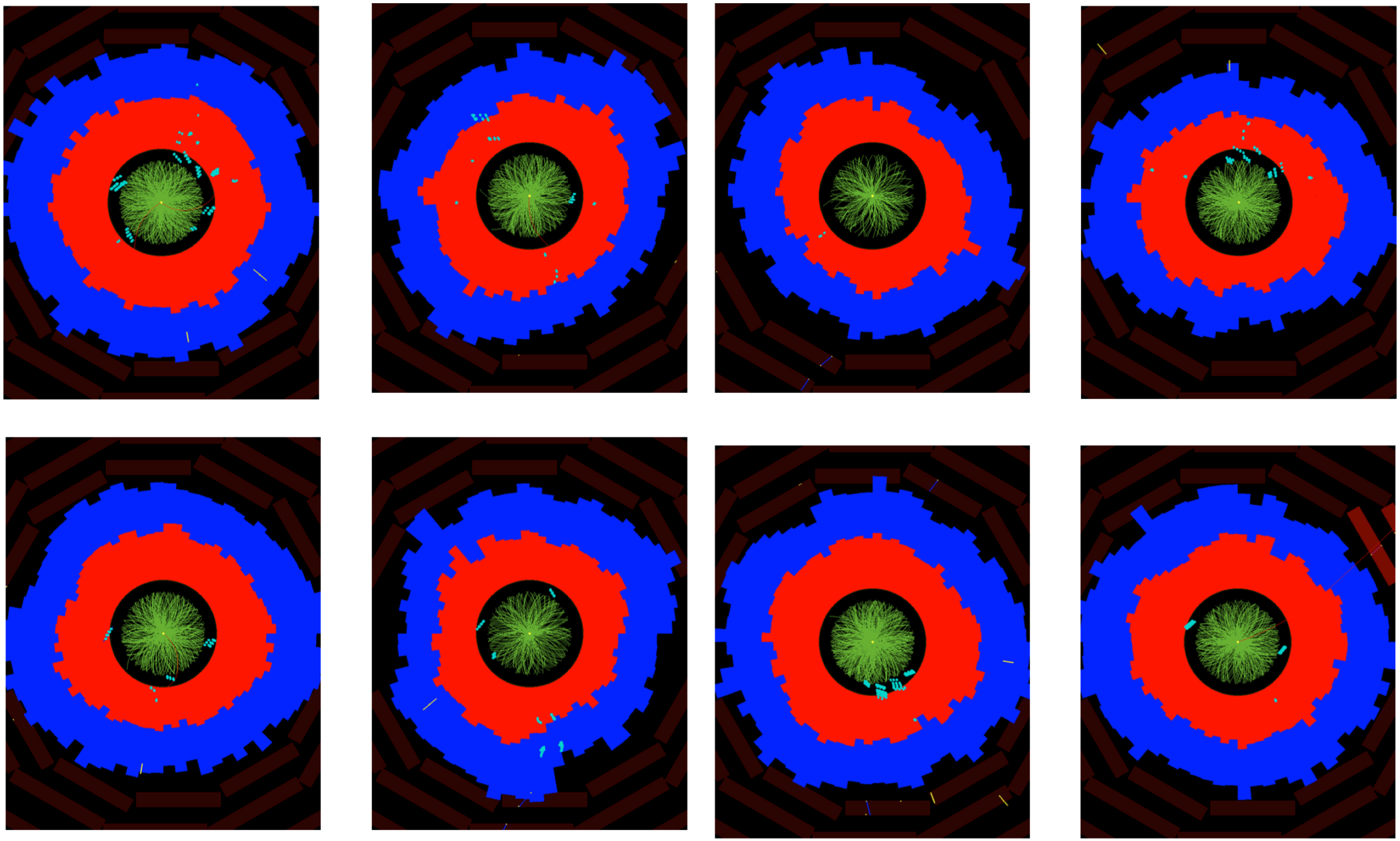

Relating final state to initial condition

$$N_{ch} \propto N_{part}$$

$$\frac{\delta[p_T]}{[p_T]} \propto -\frac{\delta R_\perp}{R_\perp}$$

$$V_n \propto \mathcal{E}_n$$

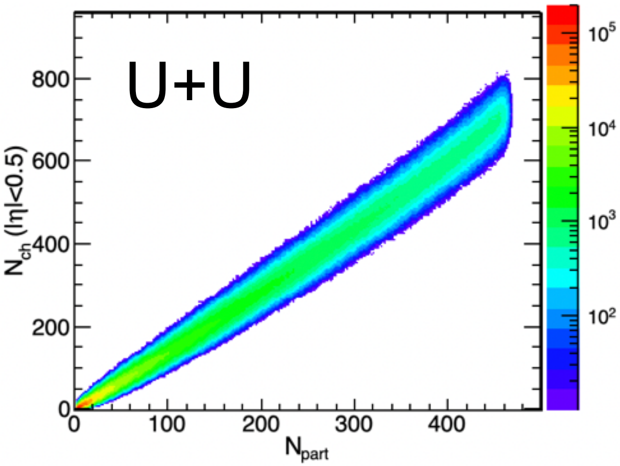

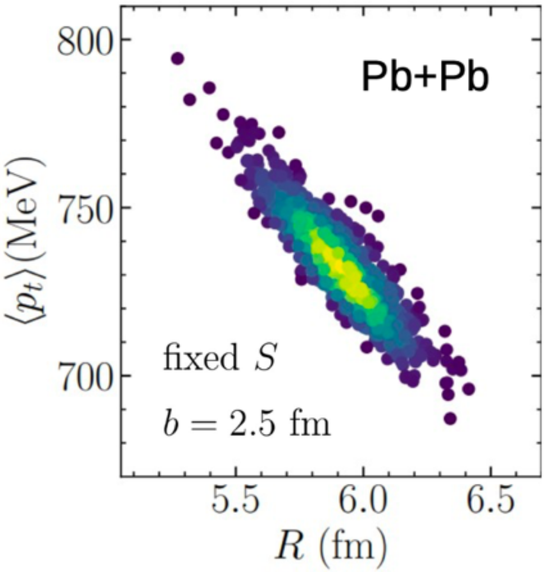

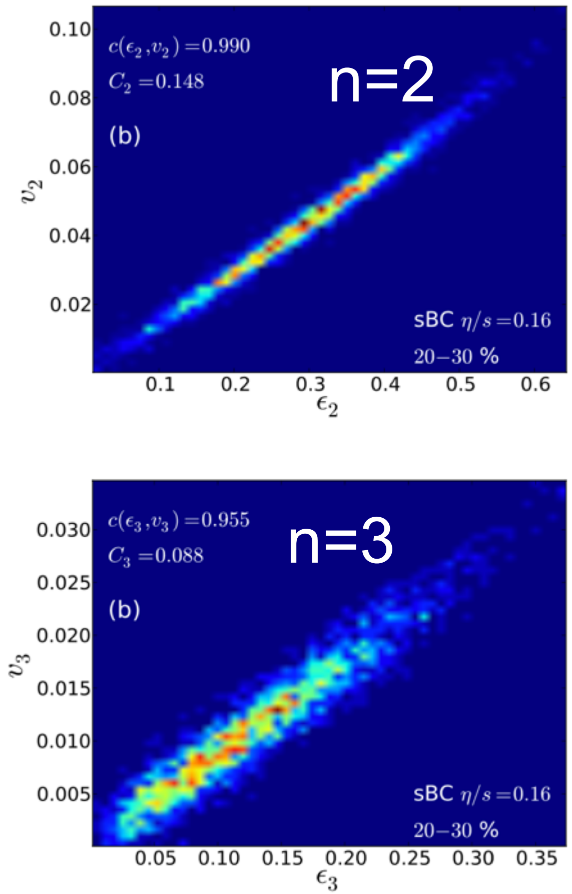

Linear correlation allows directly mapping the final state observables to geometrical properties in the initial condition

breaks down at low energy